

by Shu-zhong Shen<sup>1\*</sup>, Dong-xun Yuan<sup>2</sup>, Charles M. Henderson<sup>3</sup>, Lance L. Wardlaw<sup>4</sup>, Yi-chun Zhang<sup>5</sup>, Douglas H. Erwin<sup>6</sup>, Jahandar Ramezani<sup>7</sup>, Xiang-dong Wang<sup>1</sup>, Hua Zhang<sup>5</sup>, Qiong Wu<sup>1</sup>, Wen-qian Wang<sup>1</sup>, Jonena M. Hearst<sup>8</sup>, Jun Chen<sup>9,10</sup>, Yue Wang<sup>5</sup>, Wen-kun Qie<sup>5</sup>, Yu-ping Qi<sup>5</sup>, and Bruce R. Wardlaw<sup>11</sup>

# The Global Stratotype Section and Point (GSSP) for the base of the Capitanian Stage (Guadalupian, Middle Permian)

<sup>1</sup> State Key Laboratory for Mineral Deposits Research, School of Earth Sciences and Engineering and Frontiers Science Center for Critical Earth Material Cycling, Nanjing University, Nanjing 210023, China; Corresponding author, E-mail: szshen@nju.edu.cn

<sup>2</sup> School of Resources and Geosciences, China University of Mining and Technology, Xuzhou 221116, China

<sup>3</sup> Department of Geoscience, University of Calgary, Calgary, AB T2N 1N4, Canada

<sup>4</sup> Department of Earth and Planetary Sciences, University of Texas at San Antonio, One UTSA Circle, San Antonio, TX 78249, USA

<sup>5</sup> State Key Laboratory of Palaeobiology and Stratigraphy, Nanjing Institute of Geology and Palaeontology and Center for Excellence in Life and Paleoenvironment, Chinese Academy of Sciences, Nanjing 210008, China

<sup>6</sup> Department of Paleobiology, MRC-121, National Museum of Natural History, Washington, D.C. 20013-7012, USA

<sup>7</sup> Department of Earth, Atmospheric and Planetary Sciences, Massachusetts Institute of Technology, Cambridge, MA 02139, USA

<sup>8</sup> Guadalupe Mountains National Park, Salt Flat, TX 79847, USA

<sup>9</sup> State Key Laboratory of Isotope Geochemistry, Guangzhou Institute of Geochemistry, Chinese Academy of Sciences, Guangzhou 510640, China

<sup>10</sup>CAS Center for Excellence in Deep Earth Science, Guangzhou 510640, China

<sup>11</sup>Deceased

(Received: November 20, 2021; Revised accepted: February 10, 2022)

<https://doi.org/10.18814/epiiugs/2022/022004>

*The Global Stratotype Section and Point (GSSP) for the base of the Capitanian Stage was proposed in 1999 and defined by the first appearance datum (FAD) of the conodont Jinogondolella postserrata within the lineage J. aserrata→J. postserrata→J. shannoni at Nipple Hill in West Texas, USA. Despite its widespread recognition for more than two decades, the official GSSP paper was not published, nor have its index conodont fossils been properly documented. At Nipple Hill, only the uppermost 0.5 m of the Pinery Member belongs to the Capitanian Stage. J. postserrata first appears at 19.8 m above the base of the auxiliary Frijoles section. Based on U-Pb CA-ID-TIMS geochronology of ash beds from the GSSP area, the base of the Capitanian Stage has been constrained at 264.28±0.16 Ma. Magnetostratigraphy suggests that the Illawarra Reversal is located slightly below the base of the Capitanian Stage. Strontium isotope chemostratigraphy generally shows a continuous decline in the  $^{87}\text{Sr}/^{86}\text{Sr}$  ratio throughout the Capitanian in the GSSP area, but all ratios are higher than the Capitanian minimum of ~0.7068.  $\delta^{13}\text{C}_{\text{carb}}$  profile shows no distinct excursion around the Wordian/Capitanian boundary interval. Detailed correlation suggests that the middle-upper part of the fusuline-based Midian Stage correlates with the Capitanian Stage.*

## Introduction

The Capitanian Stage is the uppermost stage of the Guadalupian Series (Middle Permian). It has been widely documented as one of the most critical intervals of the Phanerozoic (Wardlaw, 2000; Zhou et al., 2002; Zhang et al., 2015; Shen et al., 2020). Just before the Capitanian the supercontinent Pangea shifted from assembly to a dispersal stage (Isozaki, 2009; Scotese, 2021). This continental reconfiguration was associated with large-scale volcanism represented by the massive eruption of the Emeishan basalt during the latest Capitanian in South China (Shellnutt et al., 2020; Chen and Xu, 2021). Sea level dropped to the lowest point of the Phanerozoic during the end Capitanian (Haq and Schutter, 2008), and an end-Guadalupian biological crisis has been extensively documented (Zhou et al., 2002; Clapham et al., 2009; Wignall et al., 2009; Bond et al., 2019; Chen and Shen, 2021).

The Guadalupian Series as a chronostratigraphic unit was first proposed by Girty (1902). Of the three internationally recognized component stages, the Capitanian Stage was first mentioned in a lithostratigraphic sense by Richardson (1904) for the massive reef limestones of the Guadalupe Mountains in the Delaware Basin of West Texas and New Mexico (Fig. 1A). Voting members of the Subcommission on Permian Stratigraphy (SPS) approved use of the Capitanian Stage as well as the other two stages in the Guadalupian Series, the Roadian and Wordian stages (Glenister et al., 1992, 1999; Jin et al., 1997). The GSSPs of the Roadian, Wordian and Capitanian stages of the Guadalupian

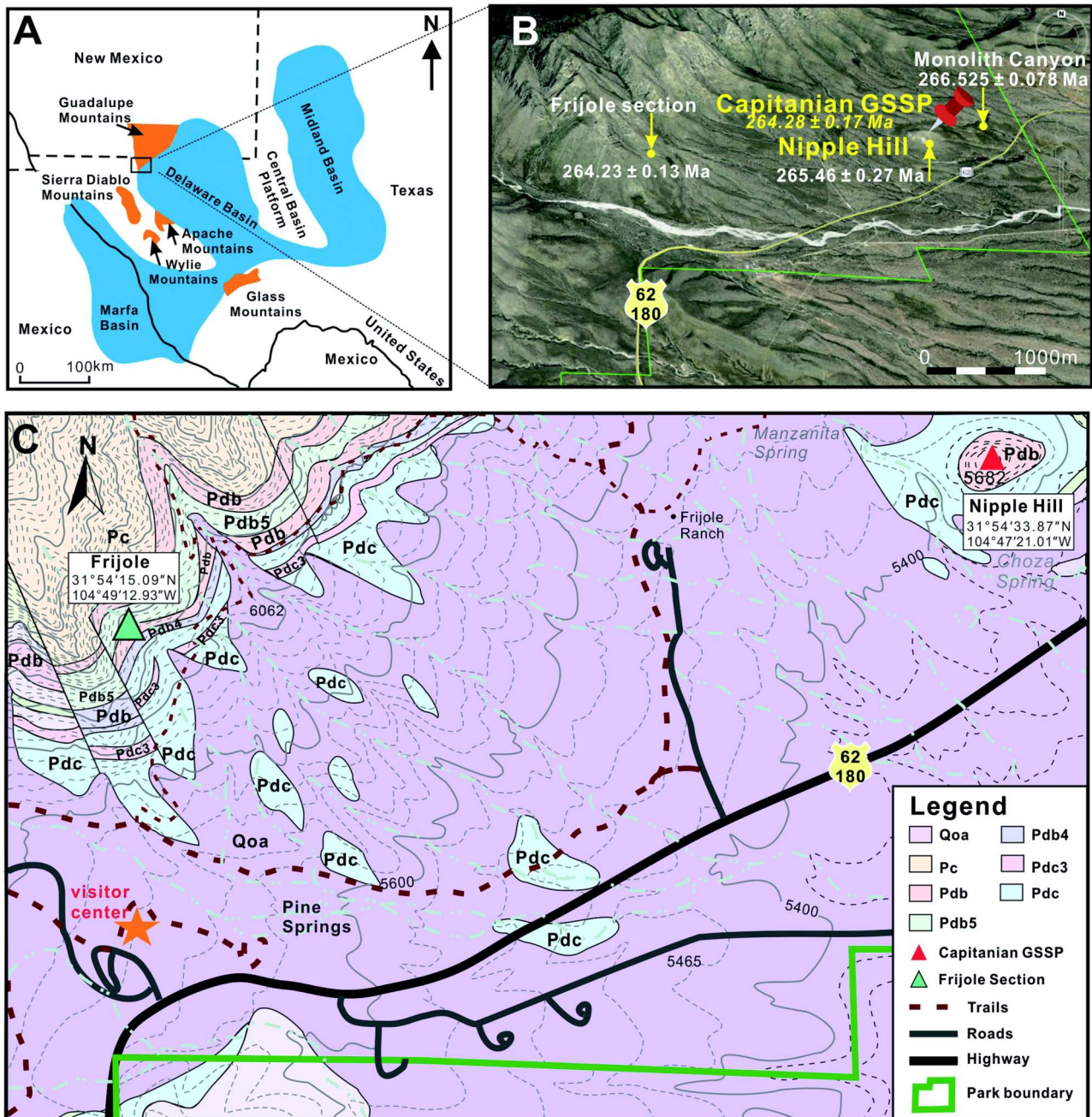


**Figure 1.** Maps showing the locations of the studied sections and topographic features in the studied area. **A**-Major structural features of the Permian Basin region in West Texas, USA showing the location of the Delaware Basin and surrounding mountains (after Harris, 2000); **B**- Google Earth image of southeastern escarpment of the Guadalupe Mountains and location of sections with radioisotopic dates; **C**-Geological map of the studied area (after King, 1948). Qoa-older alluvial deposits; Pc-Capitan Limestone; Pdb-Bell Canyon Formation; Pdb5-Pinery Member; Pdb4-Hegler Member; Pdc-Cherry Canyon Formation; Pdc3-Manzanita Member; Pdc1-Getaway Member; Pdc2-South Wells Member.

Series were proposed as international standards in the SPS Newsletter *Permophiles* by Glenister et al. (1999); the base of the Capitanian GSSP was defined by the FAD of the conodont *Jinogondolella post-serrata* within the lineage *J. aserrata*→*J. post-serrata*→*J. shannoni* in Guadalupe Mountains National Park, West Texas and New Mexico (Fig. 1). The GSSP was formally ratified in 2001 by the International Commission on Stratigraphy (ICS) and the International Union of Geological Sciences (IUGS). However, the official GSSP paper was not published, and the index conodont fossils from the Capitanian

GSSP have not been documented, although the GSSP has been widely correlated for more than two decades.

Here we correct this oversight by a detailed documentation of the Capitanian GSSP in terms of lithofacies, biostratigraphy, chemostratigraphy and radioisotope geochronology, which are the results of a six-year re-examination of the GSSP and related sections in Guadalupe Mountains National Park, as well as evaluation of the global correlation value of the Capitanian Stage.

## Location

The Capitanian GSSP is located at Nipple Hill ( $31^{\circ}54'33.87''N$ ,  $104^{\circ}47'21.01''W$ ), which is 3.45 km northeast of Guadalupe Mountains National Park Visitor Center. US Highway 62/180 passes immediately south and southeast of Nipple Hill, providing easy access. The horizontal distance from the GSSP to US Highway 62/180 is about 680 m. Nipple Hill is around 90 m high, and the GSSP is located at 0.5 m below the top of the hill (Fig. 1B, 1C). Since no further strata above the GSSP are preserved, the overlying conodont record cannot be studied at this section. Therefore, a more complete section 2.9 km to the west of the GSSP ( $31^{\circ}54'15.09''N$ ,  $104^{\circ}49'12.93''W$ ) has been studied as an auxiliary section (Fig. 1B, 1C). It has been named the Frijole section after the nearby Frijole Ranch and Museum. The steep Frijole section exposes a complete succession from the Manzanita Member (Wordian) to the Capitan Reef (Capitanian).

## Stratigraphy

Permian strata in the Guadalupe Mountains exhibit shoreline-basin

facies relationships and have been extensively studied, especially during the past half century. These strata have been critical for the development of modern sequence stratigraphy (Fig. 2) (e.g., Vail et al., 1977; Handford and Loucks, 1993; Kerans et al., 2017; Shen et al., 2020). The six composite sequences of the shelf succession are, in ascending order, the San Andres, Grayburg, Queen, Seven Rivers, Yates and Tansill formations (Glenister et al., 1992; Kerans et al., 2017). The massive reef and upper fore reef, originally called the white limestone, formed the top unit of the Guadalupian Series and was named the Capitan Limestone (Richardson, 1904). The body stratotype for the Capitan reefal limestone is situated along the western escarpment of the Guadalupe Mountains, West Texas (Figs. 1, 2). The Seven Rivers, Yates and Tansill formations occur on the shelf behind the reef tract. These formations and the Capitan Limestone are represented in the Delaware Basin by the Bell Canyon Formation, which is largely basinal sandstone, as are the underlying Cherry Canyon and Brushy Canyon formations (King, 1942, 1948; Wilde, 2000), thereby provides a shelf-to-basin correlation (Fig. 2) (Kerans et al., 2014, 2017). The Bell Canyon Formation crops out at the base of the eastern escarpment between Pine Canyon and the northeastern boundary of north US Highway 62/180, for approximately 15 km northeast of Guadalupe Peak. These outcrops provide excellent exposures of the Capitan Limestone along

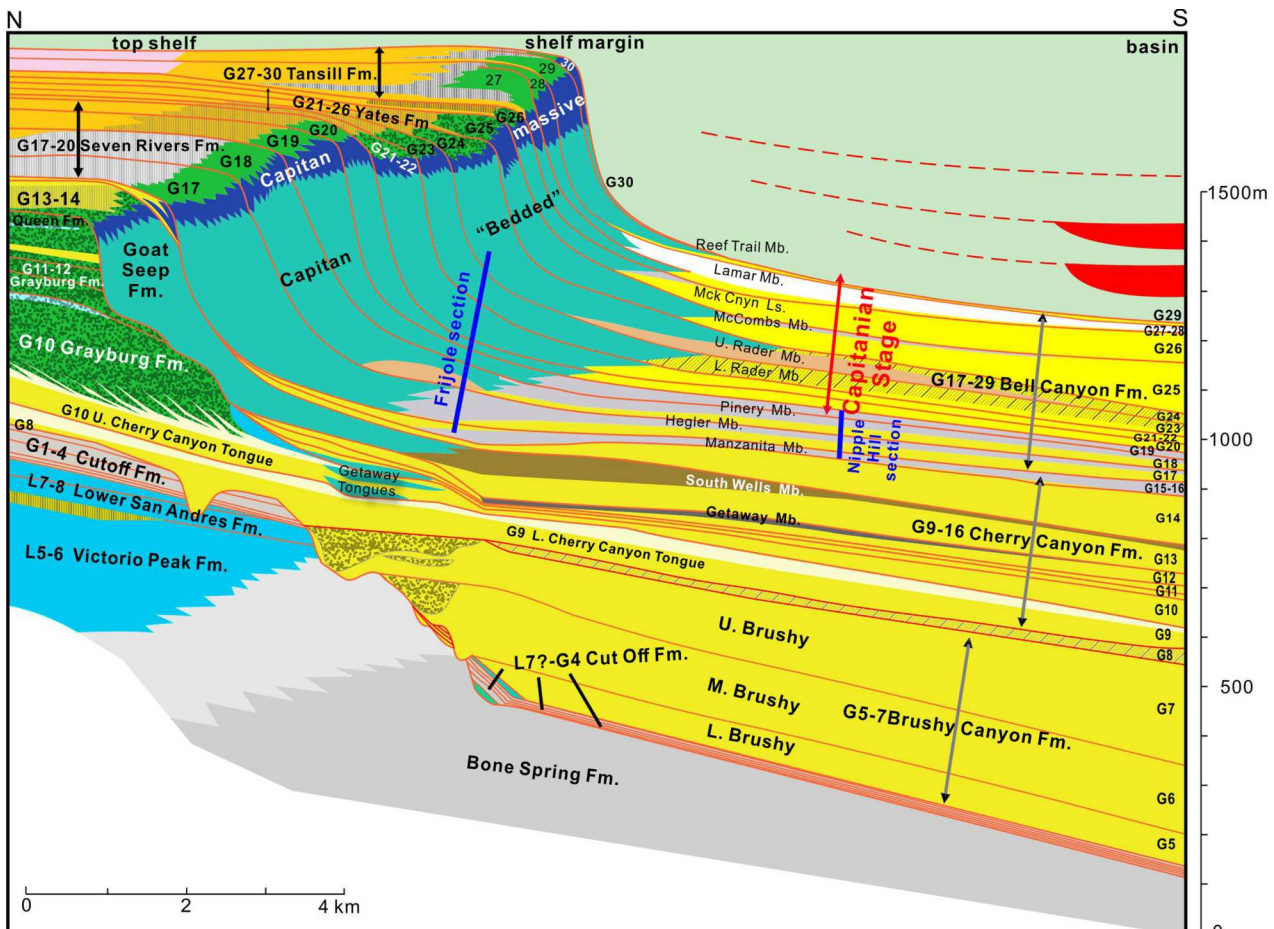


**Figure 2.** Transect across Guadalupian backreef to basin facies showing the stratigraphy, high-frequency sequences and general sedimentary settings of different lithologic units in the Guadalupe Mountains and the Delaware Basin. The extent of the defined Capitanian Stage and relative position of both studied sections are shown. Fm. = Formation; L. = lower; Ls. = limestone; M. = middle; Mb. = Member; U. = upper. L5-L8 refers to successive upper Cisuralian high-frequency sequences, and G1-G30 refers to successive Guadalupian high-frequency sequences (base figure and sequence nomenclature after Kerans et al., 2017).

the northwest margin of the Delaware Basin and unique opportunities to examine lateral and vertical changes in the Capitan Limestone along the basin margin. The succession is represented by well-exposed shelf to basinal sections in the southern Guadalupe Mountains that generally exhibit shelf evaporite, shoal-water carbonate, deep-water carbonate, and basinal sandstone facies transitions (Fig. 2).

The equivalents to the Capitan Limestone at the margin of the Delaware Basin are an alternating series of limestone and clastic members above the Manzanita Member of the Cherry Canyon Formation. The boundary marking the base of the Capitanian Stage has traditionally been drawn at the base of the Hegler Member of the Bell Canyon Formation, and includes the Hegler, Pinery, Rader, McCombs, Lamar and Reef Trail members in ascending order (Glenister et al., 1992, 1999). Following discovery of the traditional Capitanian ammonoid *Timorites* in the Manzanita Member, the boundary was lowered to the base of this member (Kerans et al., 2014; Allen and Lambert, 2017) (Fig. 2).

The base of the Capitanian Stage described in this paper as marked by the FAD of *Jinogondolella postserratata* correlates to the lowermost widespread highstand systems tract of the Seven Rivers Sequence on the shelf. In the lower slope deposition, *J. postserratata* occurs within the Pinery Limestone Member of the Bell Canyon Formation in a succession of skeletal wackestone/packstone (Figs. 2, 3). This level is much higher than the traditional basal boundary for the Capitanian Stage.

The auxiliary Frijole section exposes the uppermost Cherry Canyon Formation and the lower Bell Canyon Formation in steep outcrops nearer the Capitan Reef and therefore represents slightly shallower depositional conditions than the GSSP (Fig. 2). However, it contains much more carbonate than the GSSP at Nipple Hill. The succession is mainly composed of wackestone/packstone with chert nodules, sandstone, mudstone, and subordinate thin-bedded shale (Fig. 4). The lithostratigraphy of the Frijole section is generally consistent with the sections to the north and northwest of Nipple Hill. Following King (1948), the uppermost Manzanita Limestone Member and the lowest Hegler Limestone Member of the Bell Canyon Formation are identified near the base of the Frijole section (Fig. 4). These limestone beds are interbedded with thin sandstone and siltstone beds and occur ~15 m below the base of the Pinery Member. The correlation of the Frijole section strata to the Nipple Hill GSSP interval is slightly complicated by generally poor exposure below the Pinery Member at the two sections. The lower part of the Frijole section would either expand or condense relative to the Capitan GSSP depending on whether the carbonate unit in the middle of the Nipple Hill section correlates with the Hegler or topmost Manzanita Member (Nicklen et al., 2015b; Wu et al., 2020). However, since the Pinery Member cherty limestone is well correlated between the two sections either alternative has minimal impact on the stage boundary age interpolation. The Pinery Member as designated

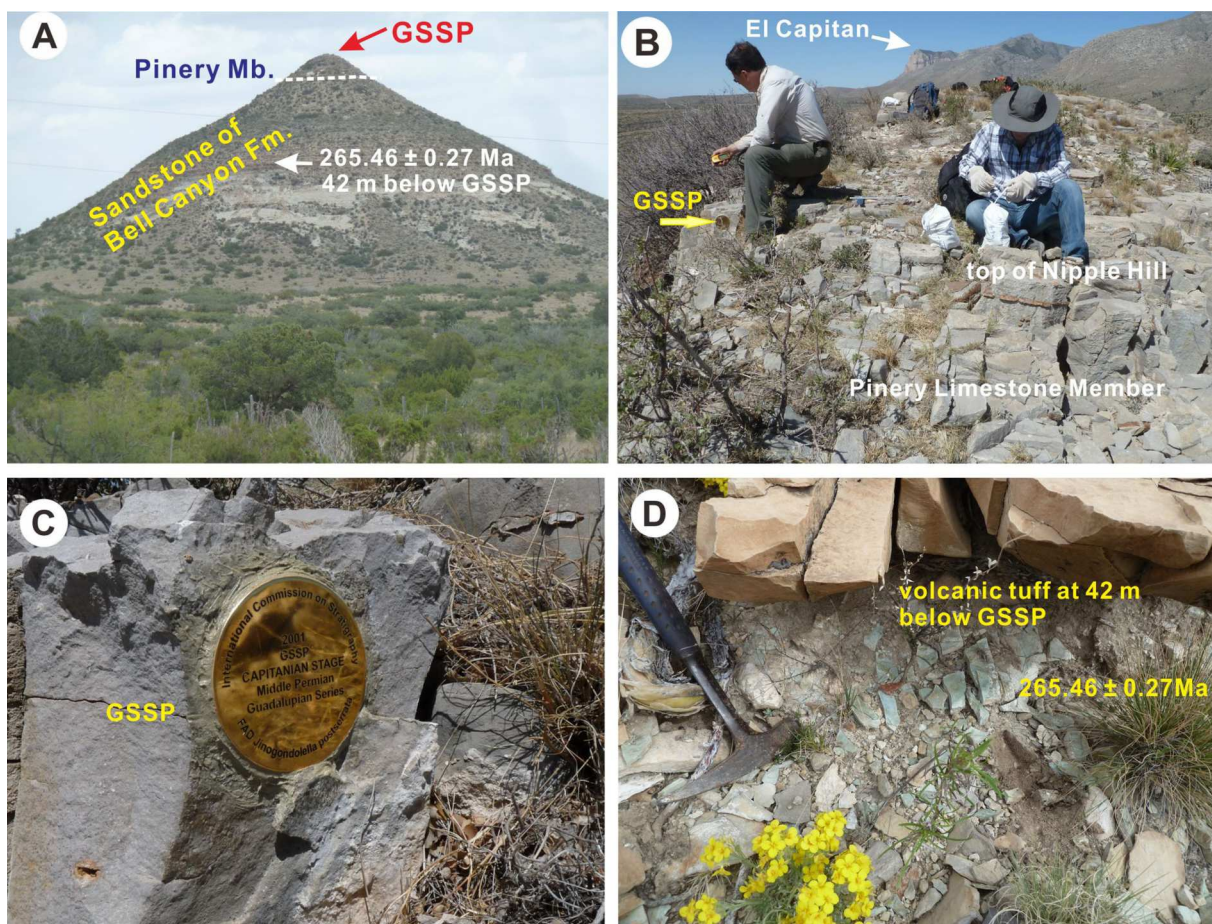


**Figure 3.** Outcrop photographs of the Capitanian GSSP section at Nipple Hill, West Texas. A-Nipple Hill, the GSSP at 0.5 m below the top of the hill; B-top of Nipple Hill showing the GSSP position in the Pinery Member; C-GSSP marker; D-a volcanic tuff dated ( $265.46 \pm 0.27$  Ma) by CA-ID-TIMS at a horizon 42 m below the GSSP at Nipple Hill.

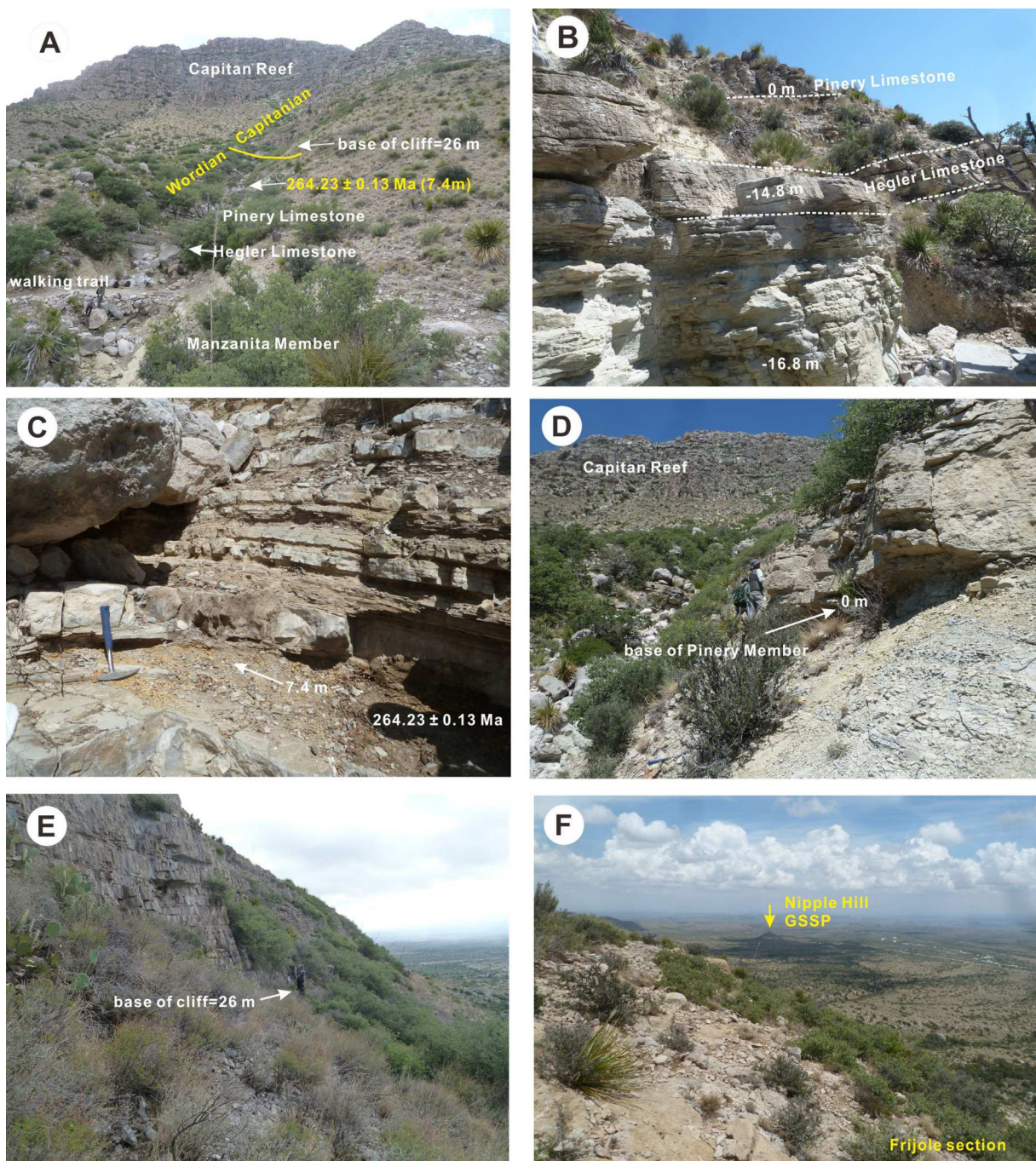


**Figure 4.** Outcrop photographs of the auxiliary Frijole section showing main lithology and stratigraphy. A- photo showing the entire Frijole section and the position of the Wordian/Capitanian boundary; B-lower part of the Frijole section showing the sandy limestone below the Hegler Member, Hegler and Pinery members in ascending order; C-A bentonite bed dated ( $264.23 \pm 0.13$  Ma) at 7.4 m above the base of the Pinery Member ; D-the base of the Pinery Member and measured 0 m at the Frijole section and the Capitan Reef in the background; E-the covered interval just above the Wordian/Capitanian boundary overlain by a cliff of the main Pinery Limestone Member based on conodont biostratigraphy; F-a view of Nipple Hill from the Frijole section.

on our figure is about 26 m thicker than that described by King (1948). When King (1948) described the Pinery Member, he did not include the interbedded sandstones and thin limestone beds between the Pinery Member and the overlying Rader Limestone (Fig. 5). We tentatively include these strata in the Pinery Member in our figure because they are partly covered at Frijole, and there are more carbonate beds in the slope depositional environment than out in the basin.

In addition, the Hegler Member is relatively thin, 5.3 m around the Nipple Hill area (King, 1948). The Pinery Member has a thickness of about 76 m at the Frijole section and it is overlain by the Rader Member, but the boundary interval between these two members is partly covered. The Rader Member is a thick-bedded limestone, with some beds containing angular limestone cobbles (King, 1948).

Detailed descriptions of the Nipple Hill (GSSP) and Frijole sec-

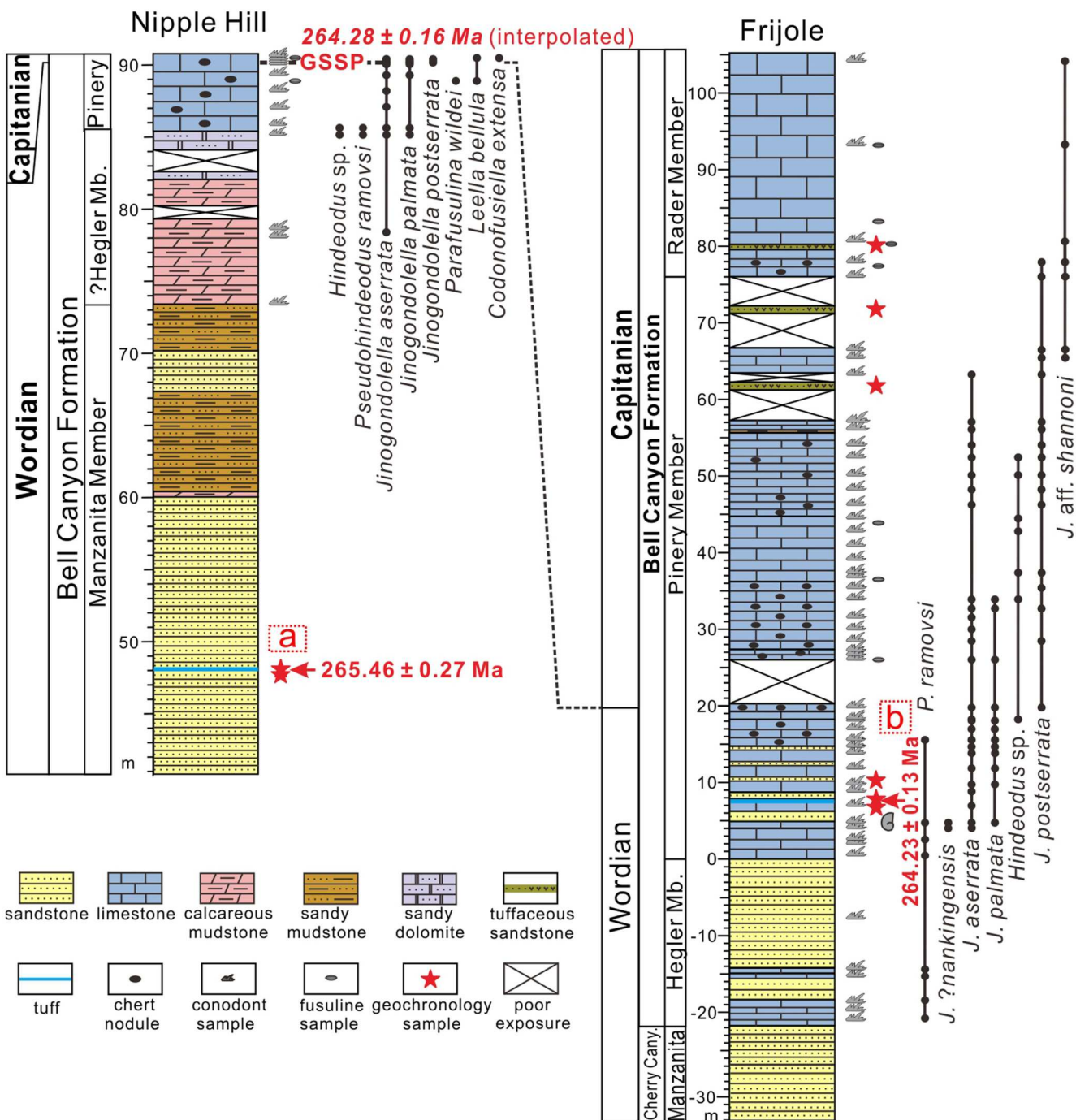


**Figure 5.** Lithostratigraphy and biostratigraphy of Nipple Hill and Frijole sections and their correlation. Question mark suggests that uncertain taxonomical identification and/or lithostratigraphy. U-Pb CA-ID-TIMS geochronology from Ramezani and Bowring (2018)<sup>a</sup> and Wu et al. (2020)<sup>b</sup> Stars without dates are samples that did not yield zircon and/or remain undated.

tions are provided in the Appendix (Figs. 3, 5).

## Biostratigraphy

### Conodonts

Eleven conodont samples were collected from the Pinery Member at Nipple Hill by Bruce Wardlaw, but no conodont specimens were

illustrated (see fig. 4 in Glenister et al., 1999). Two conodont zones are recognized around the Wordian/Capitanian boundary in this area: the *Jinogondolella aserrata* and *J. postserata* zones in ascending order (Figs. 5–9). The base of the *J. aserrata* Zone is not recognized at Nipple Hill because the sandy mudstone and sandstone about 11.5 m below the Pinery Limestone at Nipple Hill do not contain conodonts. The  $P_1$  elements of *J. aserrata* are characterized by relatively broad platforms lacking sharp anterior narrowing, shallow, poorly-defined furrows, few or no anterior serrations along its lateral platform mar-



**Figure 6.** Conodonts from the Capitanian GSSP at Nipple Hill. 1-7. *Jinogondolella aserrata* (Clark and Behnken). 1-5 from Sample NH -0.2, NIGP178098-178102; 6 from Sample NH 4.8, NIGP178103; 7 from Sample NH 4.9, NIGP178104. 8, 9. *Jinogondolella palmata* Nestell and Wardlaw, 8 from Sample NH 4.7, NIGP178105; 9 from Sample NH 0.2, NIGP178106. 10-16. *Jinogondolella postserrata* (Behnken). 10-12 from Sample NH 4.8, NIGP178107-178109; 13-16 from Sample NH 4.9, NIGP178110-178113.

gin, and a rounded posterior platform termination (typically with an inner lateral indentation). The P<sub>1</sub> elements of *J. postserrata* are char-

acterized by relatively symmetric platforms with marked anterior narrowing, sharp, well-defined furrows, common anterior serrated lateral

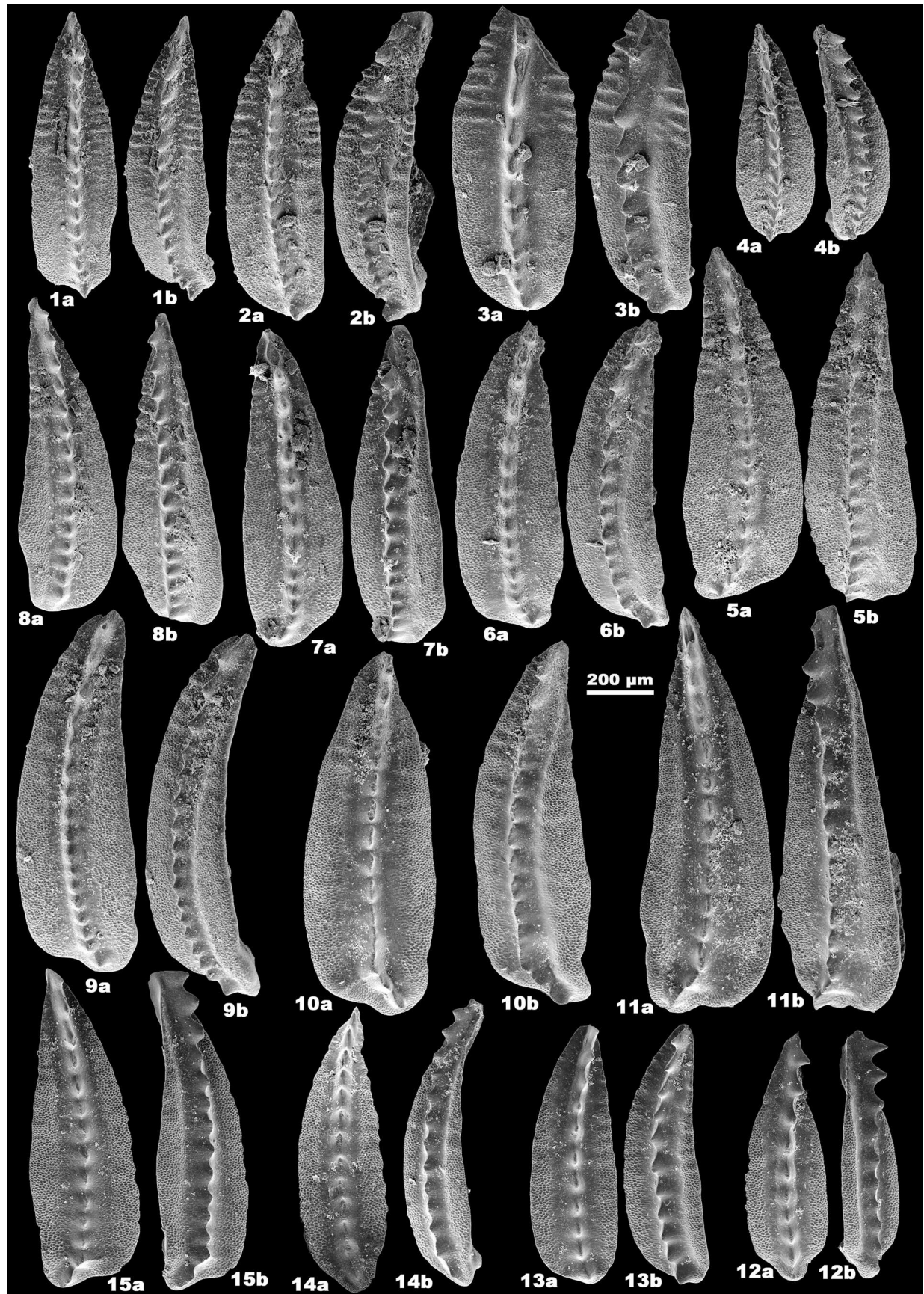


**Figure 7.** Conodonts from the auxiliary Frijole section. 1-3. *Jinogondolella* ?*nankingensis* (Jin). 1, 2 from Sample FJ 25.8, NIGP178114, 178115; 3 from Sample FJ 26.5, NIGP178116. 4-15. *Jinogondolella aserrata* (Clark and Behnken). 4 from Sample FJ 25.8, NIGP178117; 5-9 from Sample FJ 26.5, NIGP178118-178122; 10-15 from Sample FJ 30.6, NIGP178123-178128.

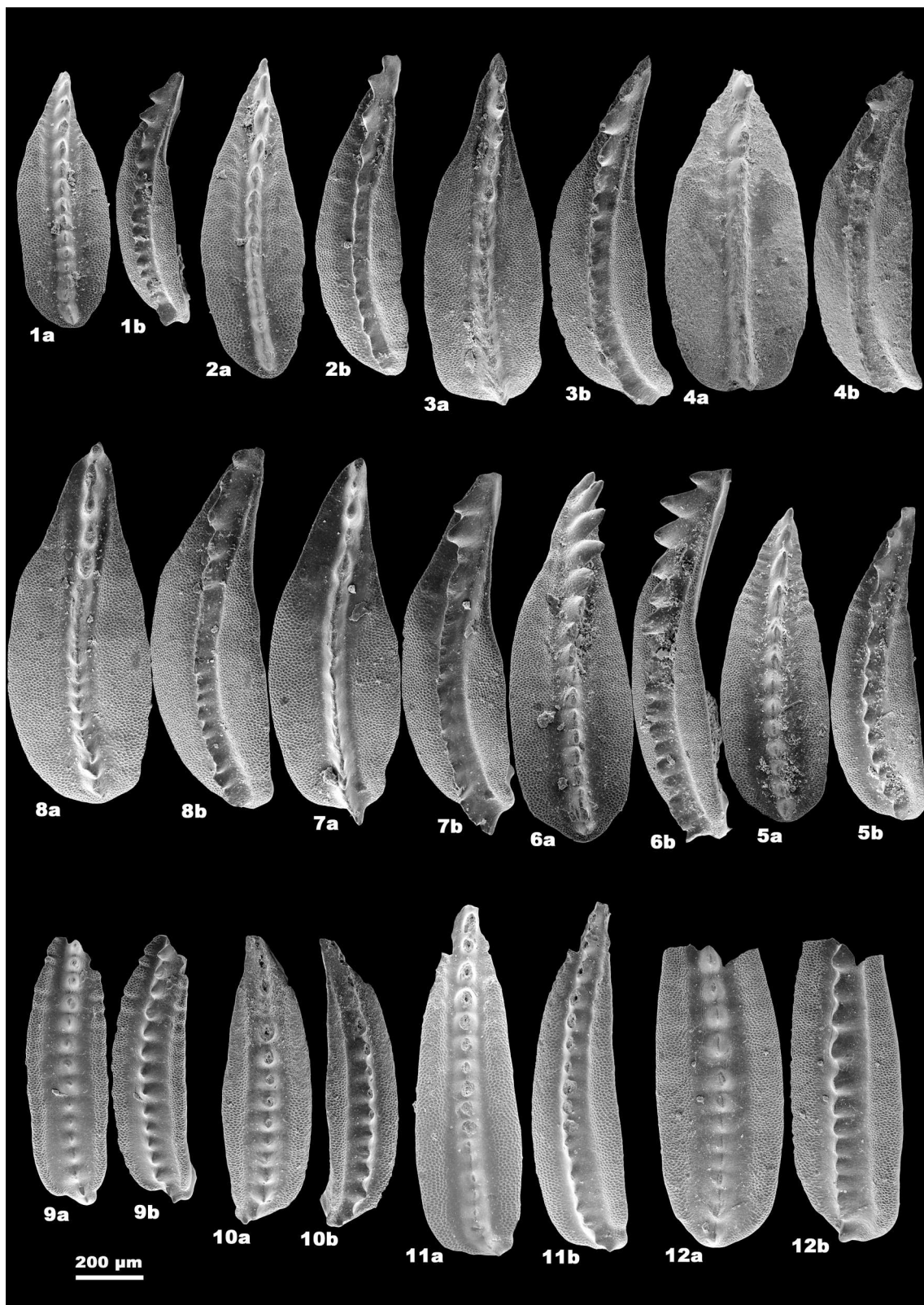


**Figure 8.** Conodonts from the auxiliary Frijole section. 1-8. *Jinogondolella palmata* Nestell and Wardlaw, from Sample FJ 35.6, NIGP178129-178136; 9-12. *Jinogondolella postserrata* (Behnken). 9-11 from Sample FJ 41.6, NIGP178137-178139; 12 from Sample FJ 50.2, NIGP178140.

margins (restricted to the anteriorly narrowing part), and relatively blunt posterior platform terminations. Transitional morphotypes from *J. aserrata* to *J. postserrata* display relatively blunt posterior termina-

tions, intermediately developed furrows, and moderately narrowing platforms in the anterior with few serrations on the margins (Wardlaw, 2000).

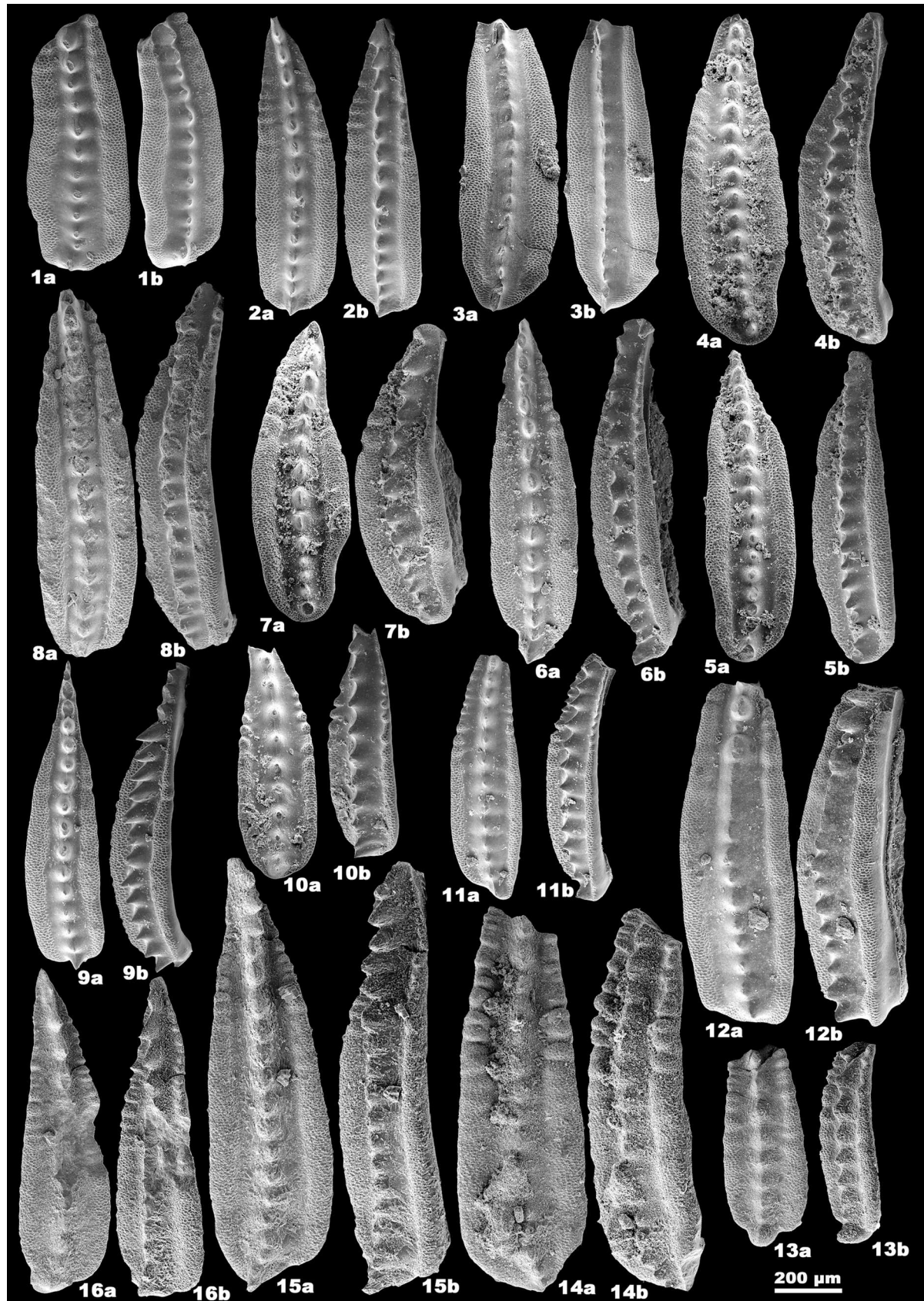


**Figure 9. Conodonts from the auxiliary Frijole section. 1-12. *Jinogondolella postserrata* (Behnken).** 1-3 from Sample FJ 68, NIGP178141-178143; 4-6 from Sample FJ 70, NIGP178144-178146; 7, 8 from Sample FJ 71.9, NIGP178147, 178148; 9, 10 from Sample FJ 75.8, NIGP178149, 178150; 11, 12 from Sample FJ 88.2, NIGP178151, 178152; 13-16. *Jinogondolella aff. shannoni* Wardlaw. from Sample FJ 115, NIGP178153-178156.

The Capitanian GSSP is defined at 90.2 m (0.5 m below the top of Nipple Hill) in the outcrop section on the south side of Nipple Hill, which coincides with the FAD of *Jinogondolella postserrata* in the Pinery Limestone Member of the Bell Canyon Formation (Figs. 3C, 5). The Pinery Member limestone at Nipple Hill contains very abundant conodonts, but sample population analysis shows that it is dominated by *J. aserrata* specimens and transitional morphotypes, and with only a few specimens in the sample population assigned to *J. postserrata*. Moreover, the *J. postserrata* Zone is only 0.5 m thick at the GSSP section. Strata above the top of Nipple Hill are not preserved

(Figs. 3B, 5).

The Frijole section is much more complete than the Nipple Hill GSSP section, but conodonts within the Wordian-Capitanian boundary interval are not as abundant as at the GSSP section. All three conodont zones can be recognized at the Frijole section. Conodonts from the horizons in the lower part of the Frijole section can be confidently assigned to the *Jinogondolella aserrata* Zone. A few specimens of *J. postserrata* occurs at 19.8 m (Figs. 5, 8), which indicates the Capitanian/Wordian boundary at the Frijole section. Unfortunately, strata between 20-26 m above the boundary are covered, and conodonts are

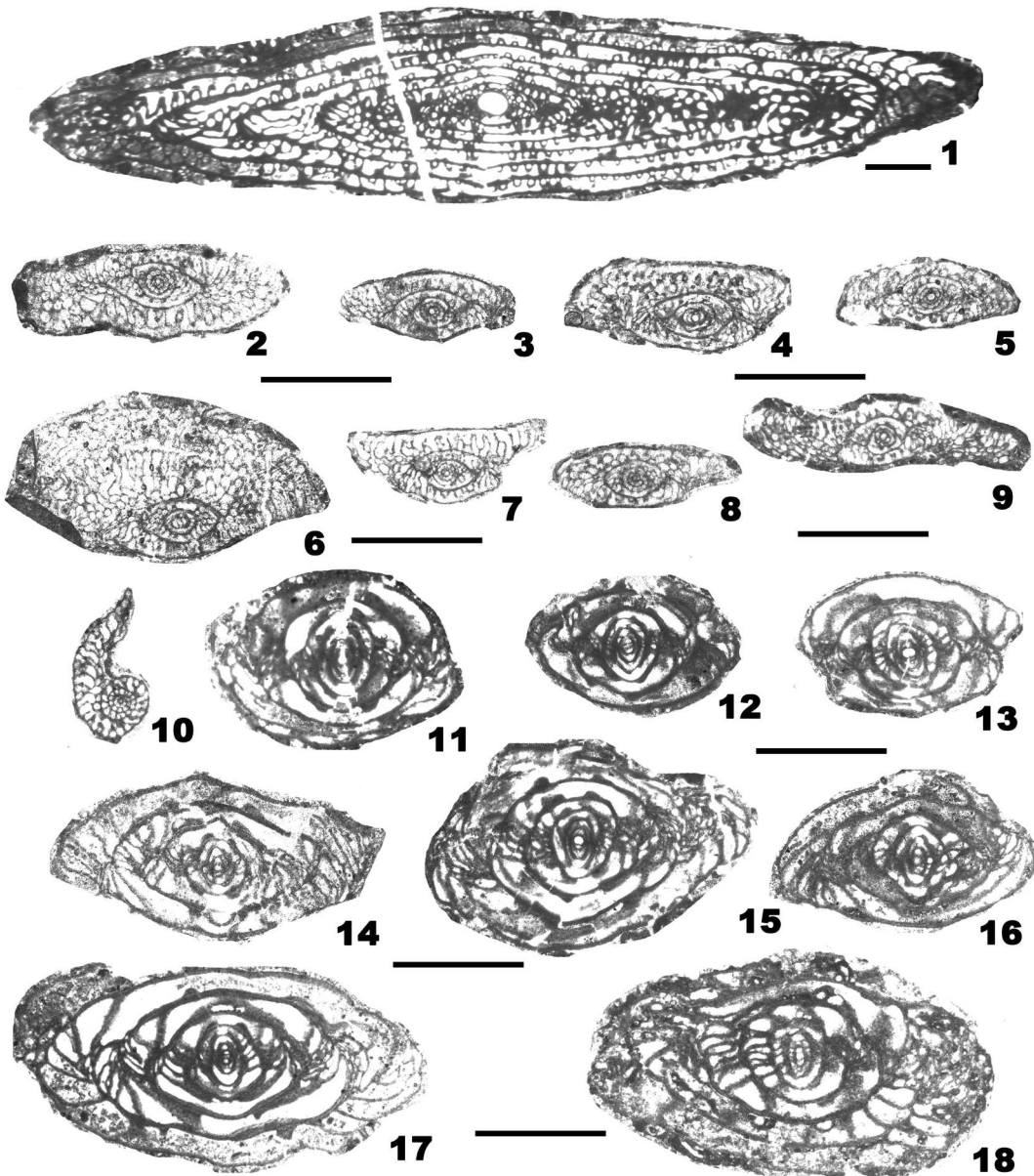


**Figure 10.** Fusulines from the Pinery Member at the Capitanian GSSP at Nipple Hill. 1-Parafusulina wildei Ross, NH 3.5-H-1, NIGP178080, axial section. 2-10. Codonofusiella extensa Skinner and Wilde. 2. NH 5.1-C-1, NIGP178081, axial section; 3. NH 5.1-T-1, NIGP178082, axial section; 4. NH 5.1-S-1, NIGP178083, axial section; 5. NH 5.1-Zb-1, NIGP178084, axial section; 6. NH 5.1-H-1, NIGP178085, axial section; 7. NH 5.1-Q-1, NIGP178086, axial section; 8. NH 5.1-F-1, NIGP178087, axial section; 9. NH 5.1-D-1, NIGP178088, axial section; 10. NH-F-D-1, NIGP178089, sagittal section. 11-18. Leella bellula Dunbar and Skinner. 11. NH 3.5-T-1, NIGP178090, axial section; 12. NH 5.1-Za-1, NIGP178091, axial section; 13. NH 3.5-B-1, NIGP178092, axial section; 14. NH 5.1-G-1, NIGP178093, axial section; 15. NH 5.1-U-1, NIGP178094, axial section; 16. NH 3.5-E-1, NIGP178095, axial section; 17. NH 3.5-U-1, NIGP178096, axial section; 18. NH 3.5-Q-1, NIGP178097, paraxial section (scale bar=1 mm).

rare between 26 m and 46.2 m. Above 46.2 m, *J. postserrata* is abundant up to the lower part of the Rader Member (Fig. 5).

In addition to the Frijole section, Wardlaw and Nestell (2015) reported a conodont succession from *Jinogondolella nankingensis behnkeni* → *J. aserrata* → *J. postserrata* in a 29 m unit (their PI section) originally mapped by King (1948) as the Pinery Limestone Member of the Bell Canyon Formation in the southern part of Patterson Hill just to the west of the Guadalupe Mountains escarpment of West Texas. This section displays a significant portion of the upper part of the Wordian in a short continuous roadcut section along US Highway 62/180, and may serve as another auxiliary section in addition to the Frijole section. However, only a few specimens of the index species *J. postser-*  
*rata* occur at 1.3 m (Sample PI-31 in Wardlaw and Nestell, 2015) below a clastic unit (Unit 14), which lacks conodonts. Thus, this section is similar to the Nipple Hill GSSP section and contains a very short part of the Capitanian Stage with conodonts. Multiple bentonitic interbeds were collected from the Patterson Hill Road cut section, but none yielded zircon (Wu et al., 2020).

### Fusulines

Fusulines below the Capitanian Stage in Guadalupe Mountains National Park are dominated by *Parafusulina* species. The two main zones of the Capitanian Stage are the *Polydiexodina* and *Paraboultonia splendens* zones. A number of subzones have been recognized within these two zones (Wilde, 2000). The lower Capitanian is characterized by *Polydiexodina*, a large fusuline with fully developed multiple tunnels, which probably evolved from a lineage of *Skinnerina* through the Asian *Eopolydiexodina* (Wilde, 1975). *Leella bellula* is associated with *Polydiexodina* and the earliest codonofusiellids (e.g., *Codonofusiella paradoxica*). Two fusuline samples were collected from the Nipple Hill GSSP section. Three species are identified. One sample 1.8 m below the top of Nipple Hill contains *Parafusulina wildei* and abundant *Leella bellula*. Wilde et al. (1999) considered that *Codonofusiella extensa* provides a useful middle Capitanian datum. This species is abundant in a sample 0.2 m below the top of Nipple Hill, therefore, *Leella bellula* has its lowest occurrence in the uppermost part of the Wordian and *Codonofusiella extensa* occurs 0.3 m above the GSSP (Figs. 5, 10).

The large and complex fusulines of the *Polydiexodina* Zone are succeeded by advanced Neoschwagerinidae. In the Guadalupe Mountains, *Paradoxiella* is followed upward by abundant *Reichelina lamarensis* (Skinner and Wilde, 1955) near the top of the Lamar Limestone Member. *Polydiexodina* ranges upward in the Capitan to the McCombs Limestone Member, then disappears. The youngest fusulines known from Guadalupe Mountains National Park are abundant *Paraboultonia* from the Reef Trail Member of the Bell Canyon Formation (Wilde, 2000). This level is correlated to the upper part of the Tansill Formation on the shelf (Fig. 2). The *Paraboultonia splendens* Zone comprises the remainder of the upper Capitanian (King, 1948; Wilde, 1990) from the upper part of the *Jinogondolella postserrata* Zone to the *J. altudaensis* and *J. prexuanhanensis* zones in the Lamar and Reef Trail members in the upper part of the Capitanian (Shen et al., 2020). Within this fusuline framework, from oldest to youngest, are the following subzones: *Yabeina texana*, *Paradoxiella pratti*, *Reichelina lamarensis*, and *Paraboultonia splendens* (Wilde, 2000; Nestell et al., 2019).

### Ammonoids

Ammonoids offer another tool for global correlation. Where found, the nektonic ammonoids are biostratigraphically reliable and were once a favored group for global correlation of the late Paleozoic. However, as nektonic microfossils, the more ubiquitous conodonts are now preferred. Up-to-date biostratigraphic ranges should be used when ammonoids are considered. The Capitanian Stage was tentatively equated to the *Timorites* Zone of Miller and Furnish (1940), although they were careful to point out that Wordian and Capitanian ammonoid faunas intergrade. At the time, the oldest known specimens of *Timorites* were recovered from the Hegler Limestone Member at the base of the Bell Canyon Formation, the traditional basal Capitanian boundary. Allen and Lambert (2017) recently pointed out that both known species of North American *Timorites* co-occur in the Manzanita Member (below the Hegler) at Casey Hill, the locus typicus of *Newellites richardsoni*. Therefore, neither genus is diagnostic of even the traditional Capitanian. Furthermore, the conodont-based Capitanian GSSP described here lies within the Pinery Member, above the Hegler Member, and well above any previously used or the currently known base of the *Timorites* Zone (Glenister et al., 1999; Davydov et al., 2018; Shen et al., 2020). Other ammonoids that are generally considered to be “Capitanian” thus also occur in the Wordian (e.g., *Cibolites uddeni* and *Nielsenoceras* (ex. *Xenaspis*) *skinneri*) (Spinoza et al. 1975).

Capitanian ammonoid faunas are now best characterized by species of *Waagenoceras* that have advanced sutures (e.g., *W. karpinskyi*). In the Guadalupe Mountains region these occur as only rare specimens in the presence of abundant *Mexicoceras guadalupense*, *Roadoceras roadense*, *Altudoceras altudense*, and *Cibolites uddeni*. As stated by Glenister et al. (1999), the Capitanian can be more easily recognized in the type Guadalupian region by the loss of ammonoids that characterize the preceding Wordian Stage. The uppermost Capitanian normal marine unit of the type Guadalupian is the Reef Trail Member, which contains *Strigogoniatis fountaini*. Ongoing research will document additional ammonoid families that are present in the Reef Trail Member.

The West Texas ammonoid record is commonly supplemented with the nearby abundant ammonoids of Las Delicias in Coahuila, Mexico. There, Capitanian ammonoids are present in the upper La Difunta and the La Colorado beds, and are more diverse than in the Guadalupe Mountains. First appearances in the upper La Difunta beds include those of *Cibolites waageni*, *Paraceltites rectangularis*, *Stacheoceras toumanskyae* and *Strigogoniatis kingi*. The upper units of the La Colorado beds contain the latest Capitanian ammonoids *Kingoceras kingi*, *Xenodiscus wanneri*, *Difuntites hidius*, *Nodosageceras nodosum* and *Eoaraxoceras ruzhencevi*. The latter four are referred to as possibly post-Guadalupian in Spinoza and Glenister (2000). The upper La Colorado ammonoid association occurs precisely as in the equivalent beds in Abadeh, central Iran and the type Dzhulfian, Transcaucasia (Spinoza and Glenister, 2000) and the third member of the Shaiwa Formation in South China (Zhou, 2017). The *Eoaraxoceras*-bearing horizons are biostratigraphically consistent in those localities, although their ultimate stage assignment will be determined by the conodont-based GSSP.

## U-Pb Geochronology

Numerous volcanic ash beds suitable for U-Pb zircon geochronology have been collected in the southern Guadalupe Mountains of West Texas (Nicklen, 2011; Nicklen et al., 2015a, 2015b; Wu et al., 2020) since they were first recognized by King (1948). One ash bed lies within the GSSP section and was originally dated by Bowring et al. (1998) using the U-Pb ID-TIMS method on multi-grain fractions of mechanically abraded zircon, yielding a weighted mean  $^{206}\text{Pb}/^{238}\text{U}$  date of  $265.3 \pm 0.2$  Ma. The ash occurs within the lower unit of the Bell Canyon Formation and 42 m below the FAD of *Jinogondolella postserrata* (Figs. 1C, 3D), and thus provides a maximum age estimate for the base of the Capitanian Stage. To verify and reinforce the age constraint for the Capitanian GSSP, Ramezani and Bowring (2018) analyzed single zircon grains from the same ash using the chemical abrasion technique (CA-ID-TIMS) and modern EARTHTIME analytical procedures and protocols, and reported a weighted mean  $^{206}\text{Pb}/^{238}\text{U}$  date of  $265.46 \pm 0.27$  Ma.

Recent U-Pb geochronology from nearby sections has significantly improved the geochronologic framework of the GSSP. About 700 m to the east-northeast of the GSSP, a 5 cm-thick greyish-green bentonite near the base of the South Wells Member of the Cherry Canyon Formation (~300 m below the GSSP) is exposed at the Monolith Canyon (Fig. 1B). Wu et al. (2020) reported a weighted mean  $^{206}\text{Pb}/^{238}\text{U}$  date of  $266.525 \pm 0.078$  Ma from this bentonite (Fig. 1B). A 4 cm-thick, buff bentonite 7.4 m above the base of the Pinery Member at the Frijole section, 2.9 km to the west of the GSSP (Figs. 1B, 4C, 5), yielded a weighted mean  $^{206}\text{Pb}/^{238}\text{U}$  date of  $264.23 \pm 0.13$  Ma, which constrains the base of the Pinery Member (Wu et al., 2020).

Nicklen (2011) reported an ash bed from the Rader Member of the Bell Canyon Formation at the Back Ridge section in the southern Guadalupe Mountains, which was dated at  $262.58 \pm 0.45$  Ma by the CA-ID-TIMS method. Another ash bed collected from the same outcrop of the Rader Member produced a weighted mean  $^{206}\text{Pb}/^{238}\text{U}$  date of  $262.127 \pm 0.097$  Ma (Wu et al., 2020), placing a minimum age constraint on the base Capitanian boundary. A Bayesian interpolation statistical algorithm was employed to construct an age-stratigraphic model for the Wordian–Capitanian strata, which yielded an interpolated age of  $264.28 \pm 0.16$  Ma for the base of the Capitanian Stage (Wu et al., 2020). Thus, the total duration for the Capitanian Stage is 4.77 Myr when the  $259.51 \pm 0.21$  Ma age of Yang et al. (2018) is used for the base of the Wuchiapingian Stage (also the top of the Capitanian Stage).

## Magnetostratigraphy

Initial magnetostratigraphic investigations within the Delaware Basin were carried out on the back-reef facies of the Guadalupe Mountains (Peterson and Nairn, 1971), with the Seven Rivers Formation demonstrating reversed polarization and normal polarity in the overlying Yates Formation. Steiner (2006) suggested that the first normal polarity magnetochron of the Illawarra Mixed Superchron appears to be shown in the middle and upper parts of the back-reef Grayburg Formation in the Guadalupe Mountains, but this was never fully documented (Lucas,

2017). In the Delaware Basin, the Grayburg Formation overlies the upper San Andres Formation and is correlative to the middle Cherry Canyon Formation. These strata contain Wordian fusulines of the *Parafusulina lineata-deliciasensis* Zone (Wilde, 1990). In terms of conodonts, the Cherry Canyon and equivalent strata of the Grayburg Formation are early and middle Wordian, in the *Jinogondolella aserrata* Zone (Yuan et al., 2021). Thus, if the beginning of the Illawarra Superchron is recorded in the Grayburg Formation, this datum is below the base of the Capitanian (Olszewski and Erwin, 2009; Hounslow and Balabanov, 2018).

Menning (2000) briefly summarized limited magnetostratigraphic data from West Texas, which led him to place the beginning of the Illawarra Superchron below the Pinery Limestone Member of the Bell Canyon Formation, just above a tuff with an age of  $265.46 \pm 0.27$  Ma (Bowring et al., 1998; Ramezani and Bowring, 2018; Shen et al., 2020). The Cutoff Formation, and the Getaway and Manzanita Limestone members of the Cherry Canyon Formation (Roadian–Wordian) exhibit reversed polarity. Thus, these units all belong to the Carboniferous–Permian Kiaman Reversed Superchron, and the existence of a few normal polarized samples in the Pinery Limestone and the Lamar Limestone confirm that the Illawarra Reversal occurs between the Manzanita Limestone and the Pinery Limestone (Steiner, 2006; Lucas, 2017). In addition, Nicklen (2011) has suggested the Queen and Grayburg formations correlate to the basinal South Wells Member of the Cherry Canyon Formation, which has an associated U–Pb (CA-ID-TIMS) date of  $266.525 \pm 0.078$  Ma in the Wordian (Wu et al., 2020).

Eight-six samples from the Capitanian GSSP section, covering 4.25 m, and 116 samples from the Apache Mountains B Section (Lambert et al., 2002), covering 5.83 m, including the Wordian–Capitanian boundary interval, were collected for magnetic susceptibility analyses (Ellwood et al., 2013). According to Ellwood et al. (2013), the magnetostratigraphic susceptibility zones are well correlated between the two sections. These zones need to be tested before they can be used for intercontinental correlation, given the different susceptibility values in the two sections.

## Cyclostratigraphy

The Guadalupian carbonate platform system in southwestern US provides an example of a ramp-to-rim transition in a carbonate to mixed siliciclastic-carbonate succession during a second-order progradational supersequence (Fig. 2). The sequence framework of the entire Guadalupian Series succession includes 30 high-frequency sequences (HFSs) deposited over a 13.64 Myr time span from the Lower San Andres Formation to the top of the Tansill Formation (Kerans et al., 2014, 2017). A total of 11 HFSs grouped into four composite sequences (CSs) were recognized from the Pinery Member to the basal part of the Castile Formation (Wilde et al., 1999; Frost et al., 2012; Kerans et al., 2014) (Fig. 2). The Rader ash age of  $262.127 \pm 0.097$  Ma (Wu et al., 2020) has been correlated to the top of HFS G23 (Kerans et al., 2017; Nicklen et al., 2015a); whereas the Monolith Canyon ash age of  $266.525 \pm 0.078$  Ma correlates with the base of HFS G14 (Kerans et al., 2014, 2017). Thus, the interval from the basal South Wells Member to the middle Rader Member encompassing 10 HFSs, was deposited during a ~4.4 Myr time span, giving each HFS

an average duration of  $\sim 0.44$  Myr, which is a little longer than the 405 Kyr long eccentricity cycle. Accordingly, the onset of the South Wells Member can be estimated at  $266.5 \pm 0.3$  Ma, the Manzanita Member at  $266.1 \pm 0.3$  Ma, the Hegler Member at  $264.8 \pm 0.3$  Ma, the Pinery Member at  $263.9 \pm 0.3$  Ma and the Rader Member at  $262.6 \pm 0.3$  Ma (Figs. 2, 11). These estimates for the bases of the limestone members are consistent with CA-ID-TIMS U-Pb dates from each unit within uncertainty (Figs. 2, 11). Assuming that the HFSs continued above the Rader Member in the same manner, the base of the Reef Trail Member would be estimated at  $259.9 \pm 0.6$  Ma (Fig. 2). The topmost part of the Reef Trail Member (G29 on Fig. 11) is estimated at  $259.5 \pm 0.7$  Ma (Wu et al., 2020). This would place the Guadalupian-Lopingian boundary at the top of HFS G29 ( $\sim 259.51 \pm 0.21$  Ma). HFS G30 shows a backstep in the reef front (Fig. 2) that indicates transgression. Prior to this level, the reef front was progradational up to the *Jinogondolella prexuanhanensis* Zone in HFS G29 – this regression is recorded in the same zone in south China (Shen et al., 2020). Above this level, the Delaware Basin became evaporitic, and no conodonts have been recovered. The Castile Formation is a varved anhydrite unit that directly overlies the normal marine Reef Trail Member, presumably because the basin quickly became restricted from open ocean circulation.

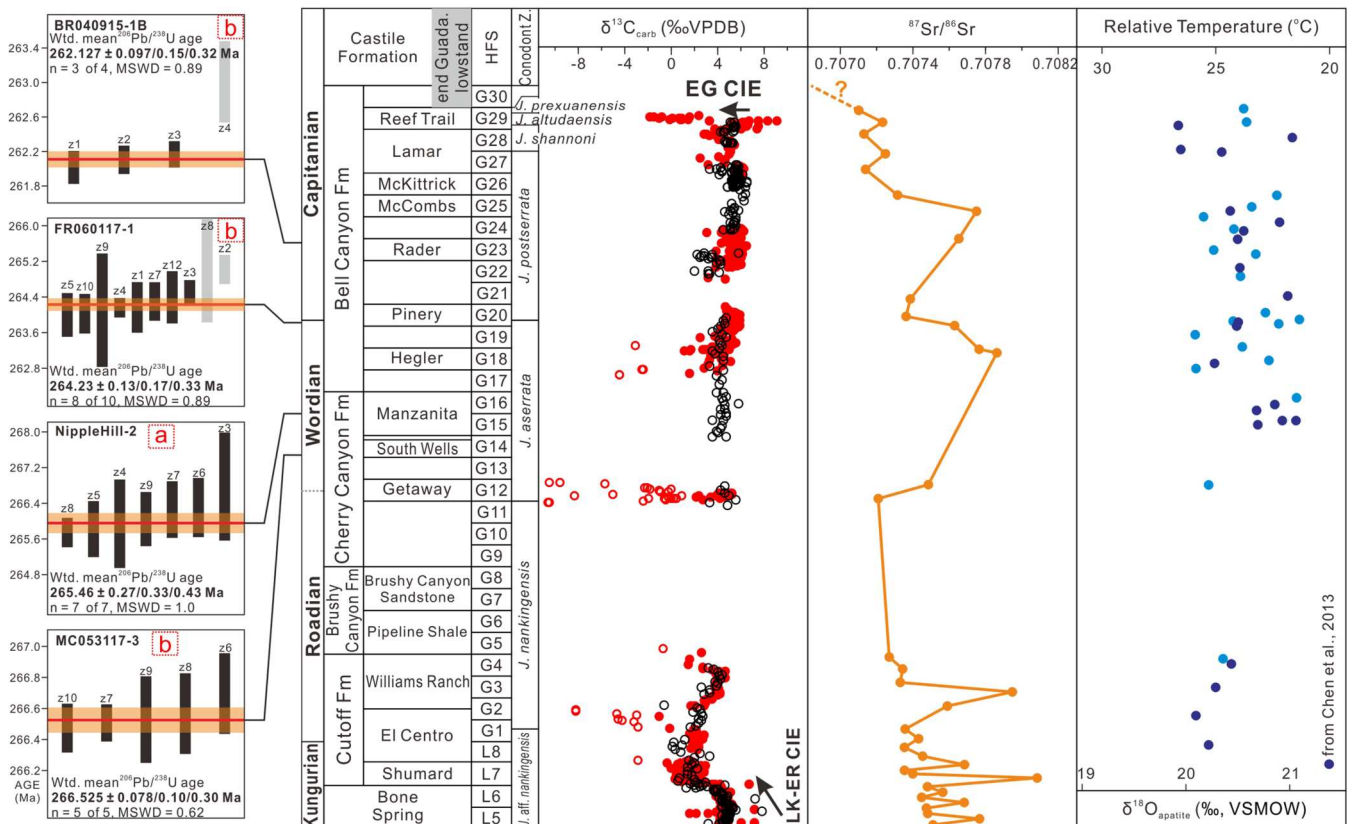


**Figure 11.**  $\delta^{13}\text{C}_{\text{carb}}$  and  $\delta^{18}\text{O}_{\text{apatite}}$ ,  ${}^{87}\text{Sr}/{}^{86}\text{Sr}$  ratio chemostratigraphy, conodont biostratigraphy, cyclostratigraphy and high-precision geochronology in the Guadalupian Series of the Guadalupe Mountains National Park. Ash bed zircon ages are from Ramezani and Bowring (2018)<sup>a</sup> and Wu et al. (2020)<sup>b</sup> and high frequency sequence stratigraphy from Kerans et al. (2014).  $\delta^{13}\text{C}_{\text{carb}}$  data in black open circle were analyzed by Werner Buggisch in GeoZentrum Nordbayern, Universität Erlangen-Nürnberg. Both the open and solid red circles were analyzed in Nanjing Institute of Geology and Palaeontology by Shen et al. (2020), of which the open circle indicates that the samples suffered diagenesis and the solid circle reflects the original signal of seawater.  $\delta^{18}\text{O}_{\text{apatite}}$  data in dark blue circle are from Chen et al. (2013) and those in pale blue are from Shen et al. (2020). HFS-high frequency sequence; EG-CIE-end Guadalupian carbon isotope excursion; Guada.-Guadalupian; LK-ER CIE-late Kungurian-early Roadian carbon isotope excursion; Z.-Zone.

## Chemostratigraphy

Only a thin carbonate interval (5.3 m in total) at the Nipple Hill GSSP section is preserved overlying sandstone of the Manzanita Member that lacks conodonts and fusulines. Therefore, it is impossible to establish a long-term chemostratigraphic framework based on the Nipple Hill GSSP section. Eighteen samples were collected from the GSSP section for carbonate carbon isotope analysis. The  $\delta^{13}\text{C}_{\text{carb}}$  values from the Pinery Limestone Member are  $3.415\text{\textperthousand}$  on average. Some values are lower to  $1.09\text{\textperthousand}$ , but there is no distinct excursion. These values are comparable with those from many sections in different regions (Shen et al., 2020). An integrative  $\delta^{13}\text{C}_{\text{carb}}$  trajectory through the entire Capitanian Stage suggests that  $\delta^{13}\text{C}_{\text{carb}}$  values remain steady through most of the Capitanian Stage until the topmost part of the upper Capitanian Reef Trail Member (upper part of the *Jinogondolella altudaensis* Zone). A large negative excursion of  $\sim 5\text{\textperthousand}$  occurs in the *J. prexuanhanensis* Zone just below the evaporite Castile Formation in the Guadalupe Mountains area (Shen et al., 2020). This negative  $\delta^{13}\text{C}_{\text{carb}}$  excursion in West Texas and New Mexico may be slightly earlier than the end-Guadalupian carbon isotope excursion in the upper part of the *J. xuanhanensis* Zone in South China (Shen et al., 2013). It is very

likely the  $\delta^{13}\text{C}_{\text{carb}}$  excursion in the top of the Reef Trail Member is due to diagenesis associated with the transition to the evaporites of the Castile Formation in the Delaware Basin (Fig. 11).

Three conodont samples collected from the Pinery Member at Nipple Hill were analyzed for  $\delta^{18}\text{O}_{\text{apatite}}$  to reconstruct paleotemperatures. Values range from 20.1‰ and 20.8‰ with an average 20.46‰, which indicates a temperature  $\sim 25^\circ\text{C}$ . The integrated  $\delta^{18}\text{O}_{\text{apatite}}$  results through the Capitanian (Chen et al., 2013; Shen et al., 2020) indicate that the  $\delta^{18}\text{O}_{\text{apatite}}$  values from the upper Kungurian throughout the Guadalupian are steady between 20–21‰ with an average value 20.5‰ in West Texas and New Mexico. No obvious Guadalupian excursion has been detected in the samples from West Texas (Fig. 11). Thus, no distinct paleotemperature changes are detected during the Capitanian.

$^{87}\text{Sr}/^{86}\text{Sr}$  ratios of two bulk samples collected at 3.3 m and 3.0 m below the top of Nipple Hill were analyzed (see methodology by Wang et al., 2018, 2021). The  $^{87}\text{Sr}/^{86}\text{Sr}$  ratios are 0.707858 and 0.707758, respectively (Shen et al., 2020) and much higher than the value 0.707047 near the Capitanian/Wordian boundary in South China (Wang et al., 2021). These high values suggest that the  $^{87}\text{Sr}/^{86}\text{Sr}$  ratios were altered by subsequent diagenesis and therefore may not be used for chemostratigraphic correlation (Fig. 11).

## Regional and Global Correlation

### Correlation with the Fusuline Biostratigraphic Framework in the Tethyan Region

Correlations between the fusuline-based biozonation in the Tethyan region and the now widely adopted conodont-based biozonation are unresolved, which limits correlation between the Tethyan and international timescales. Traditionally, the Midian Stage containing the *Yabeina-Lepidolina* Zone (Leven, 1996) was considered to be correlative with the type Capitanian Stage defined in North America. However, biostratigraphic correlation of the Capitanian Stage between Tethys and North America based on fusulines is difficult because of the high endemicity of fusulines in West Texas and New Mexico due to geo-

graphic separation by the Pangea landmass that extended from boreal to austral latitudes. The *Yabeina* Zone generally characterizes the upper Guadalupian Series in Paleotethys, but is poorly represented in West Texas and New Mexico. Several occurrences of *Yabeina* in North America were used to suggest correlations to the Paleotethys (Wilde, 2000), but these proposals are not used due to the lack of other correlation tools. In the upper Guadalupian the small, but distinctive *Yabeina texana* is well developed and is succeeded in turn by *Paradoxiella* and *Reichelina* (Skinner and Wilde, 1955). *Paradoxiella* occurs in the Paleotethys with *Yabeina globosa* (Sada and Skinner, 1977), and was reported by Leven (1993) from the Midian in Caucasus. In the Guadalupe Mountains, *Paradoxiella* is followed upward by *Reichelina* (Skinner and Wilde, 1955) near the top of the Lamar Limestone. Wilde (2000) considered that this is correlative with the late Midian *Lepidolina* Zone in the upper part of the Capitanian in Paleotethys, although the zonal index has not been found in the region.

A succession with laminated limestone turbidites and limestone slump blocks at Shigeyasu Quarry in the Akiyoshi belt, Japan contains both fusulines and volcanic ash beds. Five high-precision dates from  $265.76 \pm 0.04$  Ma to  $267.46 \pm 0.04$  Ma from the ash beds and abundant fusulines from the interbedded limestone including *Lepidolina shiraiwensis* and *Sumatrina fusiformis* in the upper Wordian Tsunemori Formation were reported (Davydov and Schmitz, 2019). The high-precision dates and the fusulines suggest that both *Lepidolina* and *Yabeina* characterize the Midian and range from upper Wordian to Capitanian. Therefore, the lower Midian is correlative with the upper Wordian, and the Capitanian Stage corresponds to only the middle-upper Midian (Zhang and Wang, 2018; Davydov and Schmitz, 2019).

### Correlation with South China

South China contains the complete Guadalupian Series, which has been named the Maokouan Subseries, and consists of the lower Kuhfengian Stage and the upper Lengwuan Stage. The Lengwuan Stage in South China has been defined to be equivalent to the Capitanian Stage of West Texas and New Mexico, USA based on the first occurrence of *Jinogondolella postserratata* (Jin et al., 1994a, 1994b; Shen et al., 2019;

West Texas, Mexico			South China						
	conodonts	ammonoids	fusulines		conodonts	ammonoids	fusulines		
Capitanian	evaporites	<i>Eoaraxoceras spinosai-Difuntites</i>	<i>Paraboultonia splendens</i> <i>Reichelina lamarensis</i> <i>Paradoxiella pratti</i> <i>Yabeina texana</i>	Lengwuan	<i>Jinogondolella granti</i>	<i>Eoaraxoceras spinosai-Difuntites furnishi</i>	<i>Lantschichites minima</i>		
	<i>J. prexuanhanensis</i>	<i>Timorites</i>			<i>J. xuanhanensis</i>	<i>Roadoceras-Doulingoceras</i>	<i>Metadolliolina multivoluta</i>		
	<i>J. altudaensis</i>				<i>J. altudaensis</i>				
	<i>J. shannoni</i>				<i>J. shannoni</i>				
Wordian	<i>J. postserratata</i>		<i>Polydiexodina</i>  <i>Parafusulina</i>	Kuhfengian	<i>J. postserratata</i>	<i>Timorites</i>	<i>Yabeina gubleri</i>		
						<i>Guixiangoceras</i>			
	<i>J. aserrata</i>	<i>Waagenoceras</i>			<i>J. aserrata</i>	<i>Waagenoceras</i>	<i>Neoschwagerina margaritae</i>		

Figure 12. Major biostratigraphic zones for correlation of upper Wordian through Capitanian strata in West Texas (and Coahuila, Mexico) and South China. Zones are shown in their relative positions. Horizontal pale grey lines indicate Wordian-Capitanian stage boundary. Angled grey line emphasizes the old ammonoid-based correlations may be diachronous. Biostratigraphic data from Shen et al. (2020).

Henderson and Shen, 2020) (Fig. 12). All the conodont zones recognized in Guadalupe Mountains National Park have been confirmed in the Maokouan Subseries in South China, and two additional conodont zones (*Jinogondolella granti* Zone and *Clarkina postbitteri hongshuiensis* Zone) lie above the *J. xuanhanensis* Zone in South China. It is still controversial among the Permian community whether these two zones are present or not in West Texas, but this is not relevant to the definition of the Capitanian GSSP (Shen et al., 2020). The lowest occurrence of *Jinogondolella postserrata* in South China is in the middle part of the carbonate Maokou Formation and the equivalent cherty Kuhfeng Formation. At the Penglaitan section, Laibin, Guangxi Province, South China, this level is ~104.6 m below the base of the Lopingian GSSP.

Ammonoids provide an additional correlation tool between South China and North America. The *Timorites* Zone has been regarded as representing the traditional Capitanian Stage, but as stated above, this genus actually occurs in the Manzanita Member. The Manzanita Member is now middle Wordian age based on the current definition of the Capitanian Stage.

The correlation between the Capitanian Stage and the cherty facies of the Lengwuan Stage has been clearly demonstrated at the Pingdingshan sections in Anhui Province, southeast China (Wu et al., 2017; Zhang et al., 2019, 2020) based on U-Pb dates. Wu et al. (2017) reported an age of  $262.2 \pm 1.7$  Ma from an ash bed at 2.5 m above the base of the Kuhfeng Formation at Pingdingshan, Anhui Province. Zhang et al. (2019) reported the dates  $261.5 \pm 1.6$  Ma from an ash bed between the Kuhfeng Formation and the overlying Yinping Formation and  $261.6 \pm 1.6$  Ma from an ash bed in the uppermost part of the Kuhfeng Formation. The top of the Capitanian Stage in South China has been intensively dated based on the Emeishan basalt (Li et al., 2017), the ash from the Wangpo Shale and claystones around the unconformity at the Maokouan-Lopingian boundary (He et al., 2010; Zhong et al., 2013; Yang et al., 2018). Currently, the CA-ID-TIMS date  $259.51 \pm 0.21$  Ma from the uppermost tuff in the Puan volcanic sequence in the eastern Emeishan large igneous province (Yang et al., 2018) constrains the timing of Emeishan volcanism and provides the reference age for the Guadalupian-Lopingian boundary (also the top of the Capitanian Stage) (Shen et al., 2020).

### **Correlation with Other Regions**

It is important to note that the serrated *Jinogondolella* lineage was increasingly restricted to paleoequatorial settings throughout the Guadalupian (Henderson, 2018). In the Phosphoria Basin of southern Idaho, USA, the youngest serrated forms are *Jinogondolella aserrata* (Wardlaw, 2015). In the Canadian Arctic, the only serrated forms are *Jinogondolella nankingensis gracilis* from the Roadian lower Assistance Formation (Henderson, 1981; Henderson and Mei, 2007). Above these datums in the northwest USA and Canadian Arctic this succession is dominated by only smooth species of *Mesogondolella* including *M. bitteri* and *M. retortensis*. Similar forms are also described from the Fantasque Formation of north-east British Columbia, Canada (Schopfer and Henderson, 2022). While the youngest age of the Great Basin and Phosphoria Basin rocks is usually indicated as Wordian (Wardlaw and Collinson, 1979; Wardlaw, 2015), Davydov et al. (2018) used geochronology to demonstrate that Phosphoria rocks extend well into the Lopingian. However, biostratigraphic correlation with West Texas

and South China is difficult because of significant provincialism.

The Capitanian Stage has long been reported in the Russian Far East (Kotlyar et al., 2007b). A widely distributed mixed fauna including ammonoids of the *Timorites* Zone and fusulines of the *Parafusulina stricta* Zone in the *Monodexodina*-beds has been found in different terranes in the Russian Far East (Kotlyar et al., 2007a; Kossovaya and Kropatcheva, 2013). The best-exposed limestone of the Chandala Formation is observed at the Senkina Shapka section in the Partizanskaya River Basin, 40 km to the north of Nakhodka. This section exceeds 200 m in thickness and is composed of well-bedded limestone with abundant and diverse fusulines, small foraminifers, bryozoans, corals, brachiopods and rare ammonoids (Kotlyar et al., 2007a). Three fusuline zones are recognized in the Chandala Formation. They are the *Monodexodina sutchanica-Metadololina dutkevitchi* Zone, the *Parafusulina stricta* Zone, and the *Metadololina lepida-Lepidolina kumaensis* Zone in ascending order. The *Metadololina lepida-Lepidolina kumaensis* Zone is associated with the conodont *Jinogondolella wilcoxi* and correlated with the Capitanian (Kotlyar et al., 2006). The *Parafusulina stricta* Zone is mostly correlated with the Capitanian because it is associated with the conodont *Jinogondolella postserrata* (Kotlyar et al., 2007a; Kani et al., 2018). Thus, the Wordian/Capitanian boundary in the Russian Far East probably lies in the lower part of the *Parafusulina stricta* Zone. Two bivalve zones, the lower *Maitaia bella* Zone and the upper *M. belliformis* Zone, are of Capitanian age based on the high-precision CA-ID-TIMS U-Pb date  $262.45 \pm 0.2$  Ma from the middle part of the Aktan Formation in the Okhotsk Massif (Davydov et al., 2018).

Capitanian carbonates of Panthalassan origin are well developed in Japan, which is represented by paleo-atoll limestones at Akasaka in Japan. The limestone was primarily deposited on a paleo-seamount in low-latitude mid-Panthalassa, and was later accreted to the eastern Pacific margin in the Jurassic (Kani et al., 2013). Extremely low  $^{87}\text{Sr}/^{86}\text{Sr}$  ratios (*ca.*  $0.7068\text{--}0.7069$ ) in the 70 m-thick Capitanian interval of the Akasaka limestone were detected. This interval with the minimum  $^{87}\text{Sr}/^{86}\text{Sr}$  ratios is around the middle Capitanian in the upper part of the *Yabeina* Zone and the *Lepidolina* Zone in Japan (Kani et al., 2008, 2013; Wang et al., 2021), but a recent study of high-precision dates from a volcanogenic siliciclastic succession containing slump limestone blocks shows that *Lepidolina* species also occur in the upper Wordian in the Akiyoshi Plateau (Davydov and Schmitz, 2019). Therefore, the *Lepidolina* Zone may be partly of late Wordian age.

The Iwaizaki Limestone formed as a patch reef within a mudstone-dominated shelf setting in the South Kitakami Belt, northeast Japan, and has been documented as representative of the Capitanian Stage in Japan (Morikawa, 1960). Nine units, Units 1-9, are subdivided in ascending order. Unit 1 consists of bioclastic limestone interbedded with sandstone, whereas the main part (Units 2-7) is composed of massive limestone with reef structures. The middle-upper part (Units 6, 7, and lower part of Unit 8) is composed of well bedded bioclastic limestone and contains the large-tested fusuline *Lepidolina multiseptata* that generally indicates a Capitanian age.

The Capitanian Stage is represented by the lower part of Wargal Formation in Salt Range, Pakistan. Units 1 and 2 contain abundant specimens of the fusuline *Sphaerulina*. *Neoschwagerina* aff. *margaritae* and *Chusenella* sp. were reported from a horizon about 5 m above the base of Unit 2 at the Chhidru Nara section (Pakistan-Japanese-Working-

Group, 1985), indicating a Capitanian age. Typical Guadalupian conodonts have not been found from the Wargal Formation in Salt Range, although complete Wuchiapingian conodont zones were reported by Wardlaw and Mei (1999) from the upper part of the Wargal Formation, which would constrain the lower part of the Wargal Formation to the Capitanian. *Neoschwagerina margaritae* has been also reported from the Surmaq Formation in the Abadeh region, central Iran, indicating the presence of the Capitanian Stage in central Iran, although detailed data are not available.

The Broughton Formation in the lower part of the Illawarra Coal Measures in the Sydney Basin, eastern Australia was traditionally assigned to the Wordian or lower stages. However, its upper part is Capitanian based on a high-precision CA-ID-TIMS date ( $263.51 \pm 0.05$  Ma) from the boundary between the Broughton Formation and Pheasants Nest Formation (Metcalfe et al., 2015). A  $^{40}\text{Ar}/^{39}\text{Ar}$  plagioclase date ( $265.05 \pm 0.46$  Ma) from the Bumbo Latite in the middle part of the Broughton Formation and the normal polarity in the Dapto Latite and Saddleback Latite marking the Illawarra Reversal also support this age determination (ca. 265 Ma, Belica et al., 2017; Shi et al., 2022). This assignment is generally supported by the  $^{87}\text{Sr}/^{86}\text{Sr}$  ratio based on brachiopod shell samples (Garbelli et al., 2019).

## Accessibility and Protection

The GSSP section on Nipple Hill is readily accessible following a short 680 m hike from US Highway 62/180. The Park Visitor Center at Pine Springs is 55 km southwest of Carlsbad, New Mexico. Access to the section begins at a slight turn to the northwest along US 62/180, 3.5 km northeast of the Pine Springs Visitor Center at Park Headquarters. The auxiliary Frijole section is more difficult to access. It is about an hour walk along the Frijole Trail from the Park Visitor Center (Fig. 1).

General collecting in United States National Parks is prohibited by law. However, specific annual permits to collect in Guadalupe Mountains National Park have been issued to qualified specialists of all nationalities, provided that specimens are to be used for scientific research purposes and that items collected are deposited in an appropriate repository that provides public access and maintains adequate museum management records. Collecting requests can be applied for through the Research Permit and Reporting System (RPRS) for the National Park Service at <https://irma.nps.gov/RPRS/>. Guadalupe Mountains National Park has designated the New Mexico Museum of Natural History and Science in Albuquerque as their partner repository for specimens. Specimens can remain with researchers while under study or other repositories under long-term storage loans if approved by the park Research Coordinator. All specimens not destroyed in analysis must be cataloged into the National Park Service Museum database.

All illustrated specimens in this paper are housed in the Nanjing Institute of Geology and Palaeontology, Chinese Academy of Sciences with a registration number prefixed by NIGP.

## Conclusions

The Capitanian GSSP is defined at Nipple Hill in Guadalupe Mountains National Park based on the FAD of the conodont *Jinogondolella postserrata*.

*doellella postserrata*. However, only 0.5 m of the Capitanian Stage is exposed in the uppermost part of the Pinery Member at this section. The Frijole section about 2.9 km west of Nipple Hill contains additional strata and provides an auxiliary reference for the Capitanian Stage. The base of the Capitanian Stage has been interpolated at  $264.28 \pm 0.16$  Ma based on radiometric dates from the Nipple Hill and Frijole sections. The middle-upper part of the fusuline-based Midian Stage in the Tethyan region correlates with the Capitanian Stage in North America.

## Appendix: Description of the sections

### Nipple Hill GSSP section (Figs. 3, 5)

#### Pinery Member of Bell Canyon Formation

85.4–90.7 m. Grey thick-bedded limestone with abundant bioclasts, conodonts, fusulinids, brachiopods, crinoids and rare cherty bands. The GSSP is at 4.8 m (measured at 90.2 m for the whole section) above the base of Pinery Member. Conodonts are dominated by *Jinogondolella aserrata* specimens in the *Jinogondolella* population, but few *J. palmata* and *J. postserrata*. Some *Pseudohindeodus ramovsi* and *Hindeodus* sp. specimens are from the sample in the base part. Identified fusulines include *Parafusulina wildei*, *Leella bellula* and *Codonofusilliella extensa* at the upper part of this limestone unit.

#### Hegler Member of Bell Canyon Formation

84.1–85.4 m. Thick-bedded sandy dolostone with cherty bands on the top of the unit. Conodonts include abundant *Jinogondolella aserrata* and some *Pseudohindeodus ramovsi* and *Hindeodus* sp. in the topmost part of this unit.

82.6–84.1 m. Not exposed.

82.2–82.6 m. Thick-bedded sandy dolostone.

80.3–82.2 m. Light grey medium-bedded calcareous mudstone.

79.4–80.3 m. Not exposed.

73.4–79.4 m. Light grey medium-bedded calcareous mudstone with numerous holes after calcite crystals were dissolved. A few *Jinogondolella aserrata* are found in a sample from the upper part of this unit.

#### Manzanita Member of Bell Canyon Formation

70.2–73.4 m. Light grey silty sandstone and sandy mudstone.

67.4–70.2 m. Light grey sandstone.

60.4–67.4 m. Light grey sandy mudstone.

60.0–60.4 m. Calcareous mudstone.

48.2–60.0 m. Light grey medium-bedded sandstone, commonly brownish when weathered.

48.0–48.2 m. A greenish volcanic tuff, ~20 cm thick (Sample no. NU-15-D-01). U-Pb ID-TIMS date of  $265.3 \pm 0.2$  Ma (Bowring et al., 1998) and CA-ID-TIMS date of  $265.46 \pm 0.27$  Ma (Ramezani and Bowring, 2018). There is another ash bed 0.5 m below this dated level. A sample (NH-15-D-01b) was collected, but has not been dated.

38.9–48.0 m. Grey medium-bedded sandstone.

0–38.9 m. Grey massive sandstone with poor bedding. No fossils found.

### The Frijole section (Fig. 5)

#### Rader Member (not measured to the top)

80.2~105.2 m. Grey thick-bedded limestone with abundant fusulines, sponges and bryozoans. Yielding conodonts *Jinogondolella* aff. *shannoni*.

79.5~80.2 m. Greyish-green tuffaceous sandstone with abundant fusulines and limestone breccia.

76.0~79.5 m. Grey thin- to medium-bedded limestone with fusulines, abundant cherty bands and nodules. Conodonts contain *Jinogondolella postserrata* and *J. aff. shannoni*.

#### Pinery Member of Bell Canyon Formation

72.2~76.0 m. Not exposed.

71.2~72.2 m. Tuffaceous sandstone.

66.7~71.2 m. Not exposed.

63.4~66.7 m. Grey thin- to thick-bedded limestone with bioclasts. A cherty band is in the basal part. Conodonts include *Jinogondolella aserrata*, *J. postserrata* and *J. aff. shannoni*.

62.2~63.4 m. Not exposed.

61.2~62.2 m. Greyish-green tuffaceous sandstone.

57.2~61.2 m. Not exposed.

56.0~57.2 m. Grey thin-bedded limestone with mudstone. Conodonts contain *Jinogondolella aserrata* and *J. postserrata*.

55.6~56.0 m. Thin-bedded mudstone and limestone.

44.7~55.6 m. Dark grey thin- to thick-bedded limestone with bioclasts, abundant cherty nodules, and thin-bedded mudstone. Conodonts contain some *Jinogondolella aserrata*, *J. postserrata* and *Hindeodus* sp.

37.5~44.7 m. Grey medium- to thick-bedded bioclastic limestone with abundant fusulines in a few beds. Conodonts include some *Jinogondolella postserrata* and *Hindeodus* sp.

26.0~35.7 m. Grey to dark grey limestone with bioclasts, cherty bands and nodules. Fusulines are found in the lower part of this unit. Conodonts contain some *Jinogondolella aserrata*, *J. palmata*, *J. postserrata* and *Hindeodus* sp.

20.0~26.0 m. Not exposed.

19.2~20.0 m. Thin-bedded limestone with abundant cherty bands or nodules. Conodonts include *Jinogondolella aserrata*, *J. palmata* and rare *J. postserrata*.

18.2~19.2 m. Grey thin-bedded limestone.

14.7~18.2 m. Grey limestone with cherty bands or nodules, and few thin-bedded sandstone. Conodonts include *Jinogondolella aserrata*, *J. palmata*, rare *Pseudohindeodus ramovsi* and *Hindeodus* sp.

8.7~14.7 m. Grey medium- to thick-bedded limestone with shale and siltstone. Conodonts include *Jinogondolella aserrata* and *J. palmata*.

7.7~8.7 m. Yellowish-brown sandstone and silty mudstone interbedded with thin limestone beds.

6.2~7.7 m. Grey medium- to thick-bedded limestone with cherty bands and thin-bedded sandstone. Conodonts include *Jinogondolella aserrata*. A buff bentonite at 7.4 m yielded a U-Pb CA-ID-TIMS date of  $264.23 \pm 0.13$  Ma (Wu et al., 2020).

5.0~6.2 m. Greenish grey sandstone with thin-bedded limestone.

0~5.0 m. Grey medium- to thick-bedded limestone with few thin-bedded silty sandstone interbedded, numerous holes after calcite crystals were dissolved and crinoids, rare brachiopods; and abundant ammonoids in the topmost part of this interval. Abundant conodont *Pseudohin-*

*deodus ramovsi* are in the lower part. Some *Jinogondolella aserrata*, a few *J. ?nankingensis*, *J. palmata* and *Pseudohindeodus ramovsi* are from conodont samples in the upper part of this unit.

#### Hegler Member of Bell Canyon Formation

(-4.6)~0 m. Yellowish-brown silty sandstone with horizontal bedding.

(-14.3)~(-4.6) m. Grey to greyish yellow silty sandstone and calcareous sandstone.

(-15.7)~(-14.3) m. Grey thin-bedded argillaceous limestone with abundant conodont *Pseudohindeodus ramovsi*.

(-18.4)~(-15.7) m. Greenish grey thin- to medium-bedded sandstone and calcareous sandstone with horizontal bedding.

(-21.8)~(-18.4) m. Grey thin-bedded sandy limestone with few crinoids and conodont *Pseudohindeodus ramovsi*.

#### Manzanita Member of Cherry Canyon Formation

(-26.5)~(-21.8) m. Grey to greyish yellow silty sandstone. No fossil found.

---

#### Acknowledgements

We sincerely thank Stanley Finney and Spencer Lucas for their very careful review and numerous useful comments to improve the manuscript. We thank Spencer Lucas for his kind assistance in shipping our large collections of the conodont samples to China. This work is supported by an international collaborative project of NSFC (Grant no. 41420104003), the Strategic Priority Research Programs of the Chinese Academy of Sciences (Grant no. XDB26000000) and the NSERC Discovery Grant to CMH.

---

#### References

- Allen, M., and Lambert, L.L., 2017, The continuing significance of Sibley Ranch localities (Culberson County, Texas) to Guadalupian (Middle Permian Series) ammonoid research. Geological Society of America Abstracts with Programs, v. 49, p. 307–14.
- Belica, M.E., Tohver, E., Pisarevsky, S.A., Jourdan, F., Denyszyn, S., and George, A.D., 2017, Middle Permian paleomagnetism of the Sydney Basin, Eastern Gondwana: Testing Pangea models and the timing of the end of the Kiaman Reverse Superchron. Tectonophysics, v. 699, pp. 178–198.
- Bond, D.P.G., Wignall, P.B., and Grasby, S.E., 2019, The Capitanian (Guadalupian, Middle Permian) mass extinction in NW Pangea (Borup Fiord, Arctic Canada): A global crisis driven by volcanism and anoxia. GSA Bulletin, v. 132, pp. 931–942.
- Bowring, S.A., Erwin, D.H., Jin, Y.G., Martin, M.W., Davidek, K., and Wang, W., 1998, U/Pb zircon geochronology and tempo of the end-Permian mass extinction. Science, v. 280, pp. 1039–1045.
- Burgess, S.D., Bowring, S.A., and Shen, S.Z., 2014, High-precision timeline for Earth's most severe extinction. Proceedings of the National Academy of Sciences, v. 111, pp. 3316–3321.
- Chen, B., Joachimski, M.M., Shen, S.Z., Lambert, L.L., Lai, X.L., Wang, X.D., Chen, J., and Yuan, D.X., 2013, Permian ice volume and palaeoclimate history: Oxygen isotope proxies revisited. Gondwana Research, v. 24, pp. 77–89.

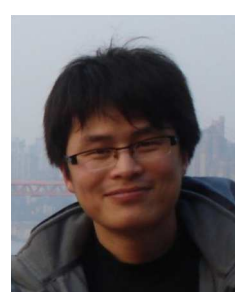
- Chen, J., and Shen, S.Z., 2021, Mid-Permian (end-Guadalupian) extinctions. In: Alderton, D., and Elias, S.A. (Eds.), Encyclopedia of Geology (Second Edition), Volume 3: United Kingdom, Academic Press, pp. 637–644.
- Chen, J., and Xu, Y.G., 2021, Permian large igneous provinces and their paleoenvironmental effects. In: Ernst, R.E., Dickson, A.J., and Bekker, A. (Eds.), Large Igneous Provinces: A Driver of Global Environmental and Biotic Changes. Geophysical Monograph 255, American Geophysical Union and John Wiley and Sons, Inc., pp. 417–434.
- Clapham, M.E., Shen, S.Z., and Bottjer, D.J., 2009, The double mass extinction revisited: reassessing the severity, selectivity, and causes of the end-Guadalupian biotic crisis (Late Permian). *Paleobiology*, v. 35, pp. 32–50.
- Davydov, V.I., Crowley, J.L., Schmitz, M.D., Snyder, W.S., 2018, New U-Pb constraints identify the end-Guadalupian and possibly end-Lopingian extinction events conceivably preserved in the passive margin of North America: Implication for regional tectonics. *Geological Magazine*, v. 155, pp. 119–131.
- Davydov, V.I., and Schmitz, M.D., 2019, High-precision radioisotopic ages for the lower Midian (upper Wordian) Stage of the Tethyan time scale, Shigeyasu Quarry, Yamaguchi Prefecture, Japan. *Palaeogeography, Palaeoclimatology, Palaeoecology*, v. 527, pp. 133–145.
- Ellwood, B.B., Lambert, L.L., Tomkin, J.H., Bell, G.L., Nestell, M.K., Nestell, G.P., and Wardlaw, B.R., 2013, Magnetostratigraphy susceptibility for the Guadalupian series GSSPs (Middle Permian) in Guadalupe Mountains National Park and adjacent areas in West Texas. *Geological Society, London, Special Publications*, v. 373, pp. 375–394.
- Frost, E.L., Budd, D.A., and Kerans, C., 2012, Syndepositional deformation in a high-relief carbonate platform and its effect on early fluid flow as revealed by dolomite patterns. *Journal of Sedimentary Research*, v. 82, pp. 913–932.
- Garbelli, C., Shen, S.Z., Immenhauser, A., Brand, U., Buhl, D., Wang, W.Q., Zhang, H., and Shi, G.R., 2019, Timing of Early and Middle Permian deglaciation of the southern hemisphere: Brachiopod-based  $^{87}\text{Sr}/^{86}\text{Sr}$  calibration. *Earth and Planetary Science Letters*, v. 516, pp. 122–135.
- Girty, G.H., 1902, The Upper Permian in western Texas. *American Journal of Science*, v. 4, pp. 363–368.
- Glenister, B.F., Boyd, D.W., Furnish, W.M., Grant, R.E., Harris, M.T., Kozur, H., Lambert, L.L., Nassichuk, W.W., Newell, N.D., Pray, L.C., Spinosa, C., Wardlaw, B.R., Wilde, G.L., and Yancey, T.E., 1992, The Guadalupian: Proposed international standard for a Middle Permian series. *International Geology Review*, v. 34, pp. 857–888.
- Glenister, B.F., Wardlaw, B.R., Lambert, L.L., Spinosa, C., Bowring, S.A., Erwin, D.H., Menning, M., and Wilde, G.L., 1999, Proposal of Guadalupian and component Roadian, Wordian and Capitanian Stages as international standards for the Middle Permian. *Permophiles*, n. 34, pp. 3–11.
- Handford, C.R., and Loucks, R.G., 1993, Carbonate depositional sequences and systems tracts - responses of carbonate platforms to relative sea-level changes. In: Loucks, R.G., and Sarg, J.F. (Eds.), Carbonate sequence stratigraphy: Recent developments and applications, American Association of Petroleum Geologists Memoir 57, American Association of Petroleum Geologists, pp. 3–42.
- Haq, B.U., and Schutter, S.R., 2008, A chronology of Paleozoic sea-level changes. *Science*, v. 322, pp. 64–68.
- He, B., Xu, Y.G., Zhong, Y.T., and Guan, J.P., 2010, The Guadalupian-Lopingian boundary mudstones at Chaotian (SW China) are clastic rocks rather than acidic tuffs: Implication for a temporal coincidence between the end-Guadalupian mass extinction and the Emeishan volcanism. *Lithos*, v. 119, pp. 10–19.
- Henderson, C.M., 1981, Conodont paleontology of the Permian Sabine Bay, Assistance and Trold Fiord Formations, northern Ellesmere Island, Canadian Arctic archipelago. MSc thesis, University of British Columbia, 135 p.
- Henderson, C.M., 2018, Permian conodont biostratigraphy. *Geological Society, London, Special Publications*, v. 450, pp. 119–142.
- Henderson, C.M., and Mei, S.L., 2007, Geographical clines in Permian and lower Triassic gondolellids and its role in taxonomy. *Palaeoworld*, v. 16, pp. 190–201.
- Henderson, C.M., and Shen, S.Z., 2020, The Permian Period. In: Gradstein, F.M., Ogg, J.G., Schmitz, M.D., and Ogg, G.M. (Eds.), *Geologic Time Scale 2020*: Amsterdam, Oxford, Cambridge, Elsevier, pp. 875–902.
- Hounslow, M.W., and Balabanov, Y.P., 2018, A geomagnetic polarity timescale for the Permian, calibrated to stage boundaries. *Geological Society, London, Special Publications*, v. 450, pp. 61–103.
- Isozaki, Y., 2009, Illawarra Reversal: The fingerprint of a superplume that triggered Pangean breakup and the end-Guadalupian (Permian) mass extinction. *Gondwana Research*, v. 15, pp. 421–432.
- Jin, Y.G., Glenister, B.F., Kotlyar, G.V., and Sheng, J.Z., 1994a, An operational scheme of Permian chronostratigraphy. In: Jin, Y.G., Utting, J., and Wardlaw, B.R. (Eds.), *Permian stratigraphy, environments and resources*, *Palaeoworld*, v. 4, pp. 1–13.
- Jin, Y.G., Zhu, Z.L., and Mei, S.L., 1994b, The Maokouan-Lopingian boundary sequences in South China. In: Jin, Y.G., Utting, J., and Wardlaw, B.R. (Eds.), *Permian stratigraphy, environments and resources*, *Palaeoworld*, v. 4, pp. 138–152.
- Jin, Y.G., Wardlaw, B.R., Glenister, B.F., and Kotlyar, C.V., 1997, Permian chronostratigraphic subdivisions. *Episodes*, v. 20, pp. 6–10.
- Kani, T., Fukui, M., Isozaki, Y., and Nohda, S., 2008, The Paleozoic minimum of  $^{87}\text{Sr}/^{86}\text{Sr}$  ratio in the Capitanian (Permian) mid-oceanic carbonates: A critical turning point in the Late Paleozoic. *Journal of Asian Earth Sciences*, v. 32, pp. 22–33.
- Kani, T., Hisanabe, C., and Isozaki, Y., 2013, The Capitanian (Permian) minimum of  $^{87}\text{Sr}/^{86}\text{Sr}$  ratio in the mid-Panthalassan paleo-atoll carbonates and its demise by the deglaciation and continental doming. *Gondwana Research*, v. 24, pp. 212–221.
- Kani, T., Isozaki, Y., Hayashi, R., Zakharov, Y., and Popov, A., 2018, Middle Permian (Capitanian) seawater  $^{87}\text{Sr}/^{86}\text{Sr}$  minimum coincided with disappearance of tropical biota and reef collapse in NE Japan and Primorye (Far East Russia). *Palaeogeography, Palaeoclimatology, Palaeoecology*, v. 499, pp. 13–21.
- Kerans, C., Playton, T., Phelps, R., and Scott, S.Z., 2014, Ramp to rimmed shelf transition in the Guadalupian (Permian) of the Guadalupe Mountains, West Texas and New Mexico. In: Verwer, K. (Ed.), *Deposits, Architecture, and Controls of Carbonate Margin, Slope and Basinal Settings*. SEPM Society for Sedimentary Geology, Special Publication No.105, Volume 105: Tulsa, SEPM Society for Sedimentary Geology, pp. 26–49.
- Kerans, C., Zahm, C., Garcia-Fresca, B., and Harris, P., 2017, Guadalupe Mountains, West Texas and New Mexico: Key excursions. *AAPG Bulletin*, v. 101, pp. 465–474.
- King, P.B., 1942, Permian of West Texas and Southeastern New Mexico. *American Association of Petroleum Geologists Bulletin*, v. 26, pp. 533–763.
- King, P.B., 1948, Geology of the southern Guadalupe Mountains Texas. *Geological Survey Professional Paper* 215, p. 183.
- Kossovaya, O.L., and Kropatcheva, G.S., 2013, Extinction of Guadalupian rugose corals: An example of biotic response to the Kamura event (southern primorye, Russia). *Geological Society Special Publication*, v. 376, pp. 407–429.
- Kotlyar, G.V., Belyansky, G.C., Burago, V.I., Nikitina, A.P., Zakharov, Y.D., and Zhuravlev, A.V., 2006, South Primorye, Far East Russia-A key region for global Permian correlation. *Journal of Asian Earth Sciences*, v. 26, pp. 280–293.
- Kotlyar, G.V., Kossovaya, O., and Zhuravlev, A., 2007a, Late Wordian-Capitanian mixed faunas of East Asia. In: *Proceedings Proceedings of the XVth International Congress on Carboniferous and Permian Stratigraphy*, Utrecht of Netherland, Royal Netherlands Academy of Arts and Sciences, Amsterdam, pp. 537–545.

- Kotlyar, G.V., Shen, S.Z., Kossovaya, O.L., and Zhuravlev, A.V., 2007b, Middle Permian (Guadalupian) biostratigraphy in South Primorye, Russian Far East and correlation with Northeast China. *Palaeoworld*, v. 16, pp. 173–189.
- Lambert, L.L., Wardlaw, B.R., Nestell M.K., and Nestell, G.P., 2002, Latest Guadalupian (Middle Permian) conodonts and foraminifers from West Texas. *Micropaleontology*, v. 48, pp. 343–364.
- Lambert, L.L., Wardlaw, B.R., and Henderson, C.M., 2007, *Mesogondolella* and *Jinogondolella* (Conodonta): Multielement definition of the taxa that bracket the basal Guadalupian (Middle Permian Series) GSSP. *Palaeoworld*, v. 16, pp. 208–221.
- Lambert, L.L., Bell, G.L., Fronimos, J.A., Wardlaw, B.R., and Yisa, M.O., 2010, Conodont biostratigraphy of a more complete Reef Trail Member section near the type section, latest Guadalupian Series type region. *Micropaleontology*, v. 56, pp. 233–253.
- Leven, E.Y., 1993, Sumatriniid phylogeny and the question of the zonal subdivisions of the Murghabian and Midian stages of the Permian. *Paleontologicheskii Zhurnal*, n. 3, pp. 23–29.
- Leven, E.Y., 1996, The Midian Stage of the Permian and its boundaries. *Stratigraphy and Geological Correlation*, v. 4, pp. 540–551.
- Li, Y.J., He, H.Y., Ivanov, A.V., Demontrova, E.I., Pan, Y.X., Deng, C.L., Zheng, D.W., and Zhu, R.X., 2017,  $^{40}\text{Ar}/^{39}\text{Ar}$  age of the onset of high-Ti phase of the Emeishan volcanism strengthens the link with the end-Guadalupian mass extinction. *International Geology Review*, v. 60, pp. 1906–1917.
- Lucas, S.G., 2017, Identification and age of the beginning of the Permian-Triassic Illawara Superchron. *Permophiles*, n. 65, pp. 11–14.
- Menning, M., 2000, Magnetostratigraphic results from the Middle Permian type section, Guadalupe Mountains, West Texas. *Permophiles*, v. 37, p. 16.
- Metcalfe, I., Crowley, J.L., Nicoll, R.S., and Schmitz, M., 2015, High-precision U-Pb CA-TIMS calibration of Middle Permian to Lower Triassic sequences, mass extinction and extreme climate-change in eastern Australian Gondwana. *Gondwana Research*, v. 28, pp. 61–81.
- Miller, A.K., and Furnish, W.M., 1940, Permian ammonoids of the Guadalupe Mountain region and adjacent areas. *Geological Society of America Special Papers*, v. 26, pp. 1–238.
- Morikawa, R., 1960, Fusulinids from the Iwaizaki limestone. *Science Reports of the Saitama University, Series B*, v. 3, pp. 273–299.
- Nestell, M.K., Nestell, G.P., and Wardlaw, B.R., 2019, Integrated Fusulinid, Conodont, and Radiolarian Biostratigraphy of the Guadalupian (Middle Permian) in the Permian Basin Region, USA. Chapter 8. In: Ruppel, S.C. (Ed.), *Anatomy of a Paleozoic Basin, the Permian Basin, USA (vol. 1)*: The University of Texas at Austin, Bureau of Economic Geology Report of Investigations 285, AAPG Memoir 118, pp. 251–291.
- Nicklen, B.L., 2011, Establishing a Tephrochronologic Framework for the Middle Permian (Guadalupian) Type Area and Adjacent Portions of the Delaware Basin and Northwestern Shelf, West Texas and Southeastern New Mexico, USA, PhD dissertation, University of Cincinnati, 119 p.
- Nicklen, B.L., Bell, G.L.J., and Huff, W.D., 2015a, A new shelf-to-basin timeline for the Middle Permian (Guadalupian) Capitan depositional System, West Texas and southeastern New Mexico, USA. *Stratigraphy*, v. 12, pp. 109–122.
- Nicklen, B.L., Bell, G.L.J., Lambert, L.L., and Huff, W.D., 2015b, Tephrochronology of the Manzanita Limestone in the Middle Permian (Guadalupian) Type Area, West Texas and southeastern New Mexico, USA. *Stratigraphy*, v. 12, pp. 123–147.
- Olszewski, T.D., and Erwin, D.H., 2009, Change and stability in Permian brachiopod communities from western Texas. *Palaios*, v. 24, pp. 27–40.
- Pakistan-Japanese-Working-Group, 1985, Permian and Triassic Systems in the Salt Range and Surghar Range, Pakistan. In: Nakazawa, K., and Dickins, J.M. (Eds.), "The Tethys" her paleogeography and paleobiogeography from Paleozoic to Mesozoic, Tokyo, Tokai University Press, pp. 221–312.
- Peterson, D.N., and Nairn, A.E.M., 1971, Palaeomagnetism of Permian Redbeds from the South-western United States. *Geophysical Journal International*, v. 23, pp. 191–205.
- Ramezani, J., and Bowring, S.A., 2018, Advances in numerical calibration of the Permian timescale based on radioisotopic geochronology. *Geological Society, London, Special Publications*, v. 450, pp. 51–60.
- Richardson, G.B., 1904, Report of a reconnaissance in Trans-Pecos Texas. *University of Texas, Mineral Survey Series, Bulletin*, v. 9, pp. 1–119.
- Sada, K., and Skinner, J.W., 1977, *Paradoxiella* from Japan. *Journal of Paleontology*, v. 38, pp. 311–315.
- Schoepfer, S.D., and Henderson C.M., 2022, Paleogeographic implications of open-marine anoxia in the Permian-Triassic Slide Mountain Ocean. In: Henderson C.M., Ritter S., and Snyder W.S. (Eds.), Late Paleozoic and Early Mesozoic Tectonostratigraphy and Biostratigraphy of Western Pangea, Society for Sedimentary Geology (SEPM), Special Publication, v. 113, in press.
- Scotese, C.R., 2021, An atlas of Phanerozoic paleogeographic maps: The seas come in and the seas go out. *Annual Review of Earth and Planetary Sciences*, v. 49, pp. 679–728.
- Shellnutt, J.G., Pham, T.T., Denyszyn, S.W., Yeh, M.W., and Tran, T.A., 2020, Magmatic duration of the Emeishan large igneous province: Insight from northern Vietnam. *Geology*, v. 48, pp. 457–461.
- Shen, S.Z., Cao, C.Q., Zhang, H., Bowring, S.A., Henderson, C.M., Payne, J.L., Davydov, V.I., Chen, B., Yuan, D.X., Zhang, Y.C., Wang, W., and Zheng, Q.F., 2013, High-resolution  $\delta^{13}\text{C}_{\text{carb}}$  chemostratigraphy from latest Guadalupian through earliest Triassic in South China and Iran. *Earth and Planetary Science Letters*, v. 375, pp. 156–165.
- Shen, S.Z., Zhang, H., Zhang, Y.C., Yuan, D.X., Chen, B., He, W.H., Mu, L., Lin, W., Wang, W.Q., Chen, J., Wu, Q., Cao, C.Q., Wang, Y., and Wang, X.D., 2019, Permian integrative stratigraphy and timescale of China. *Science in China Series D: Earth Sciences*, v. 62, pp. 154–188.
- Shen, S.Z., Yuan, D.X., Henderson, C.M., Wu, Q., Zhang, Y.C., Zhang, H., Mu, L., Ramezani, J., Wang, X.D., Lambert, L.L., Erwin, D.H., Hearst, J.M., Xiang, L., Chen, B., Fan, J.X., Wang, Y., Wang, W.Q., Qi, Y.P., Chen, J., Qie, W.K., and Wang, T.T., 2020, Progress, problems and prospects: An overview of the Guadalupian Series of South China and North America. *Earth-Science Reviews*, v. 211, pp. 103412.
- Shi, G.R., Nutman, A.P., Lee, S.M., Jones, B.G., and Bann, G., 2022, Reassessing the chronostratigraphy and tempo of climate change in the Lower-Middle Permian of the southern Sydney Basin, Australia: Integrating evidence from UPb zircon geochronology and biostratigraphy. *Lithos*, v. 410–411, pp. 106570.
- Skinner, J.W., and Wilde, G.L., 1955, New fusulinids from the Permian of West Texas. *Journal of Paleontology*, v. 29, pp. 927–940.
- Spinoza, C., Furnish, W.M., and Glenister, B.F., 1975, The Xenodiscidae, Permian ceratitoid ammonoids. *Journal of Paleontology*, v. 49, pp. 239–283.
- Spinoza, C., and Glenister, B.F., 2000, Ancestral Araxoceratinae (Upper Permian Ammonoidea) from Mexico and Iran. In: Wardlaw, B.R., Grant, R.E., and Rohr, D.M. (Eds.), *The Guadalupian Symposium, Smithsonian Contributions to the Earth Sciences*, n. 32, pp. 397–406.
- Steiner, M.B., 2006, The magnetic polarity time scale across the Permian-Triassic boundary. In: Lucas, S.G., Cassinis, G., and Schneider, J.W. (Eds.), *Non-marine Permian biostratigraphy and biochronology*, The Geological Society, London, v. 265, pp. 15–38.
- Vail, P.R., Mitchum, R.M.J., and Thompson, S., 1977, Seismic stratigraphy and global changes in sea level. In: Payton, C.E. (Ed.), *Seismic Stratigraphy-Applications to Hydrocarbon Exploration*: American Association of Petroleum Geologists Memoir 26: Tulsa, American Association of Petroleum Geologists, pp. 83–97.
- Wang, W.Q., Garbelli, C., Zheng, Q.F., Chen, J., Liu, X.C., Wang, W., and Shen, S.Z., 2018, Permian  $^{87}\text{Sr}/^{86}\text{Sr}$  chemostratigraphy from carbonate sequences in South China. *Palaeogeography, Palaeoclimatology, Palaeoecology*, v. 500, pp. 84–94.
- Wang, W.Q., Katchinoff, J.A.R., Garbelli, C., Immenhauser, A., Zheng,

- Q.F., Zhang, Y.C., Yuan, D.X., Shi, Y.K., Wang, J.Y., Planavsky, N., and Shen, S.Z., 2021, Revisiting the Permian seawater  $^{87}\text{Sr}/^{86}\text{Sr}$  record: New perspectives from brachiopod proxy data and stochastic oceanic box models. *Earth-Science Reviews*, v. 218, pp. 103679.
- Wardlaw, B.R., 2000, Guadalupian conodont biostratigraphy of the Glass and Del Norte Mountains. In: Wardlaw, B.R., Grant, R.E., and Rohr, D.M. (Eds.), *The Guadalupian Symposium, Smithsonian contributions to the Earth Sciences*, Washington D.C., Smithsonian Institution, n. 32, pp. 37–81.
- Wardlaw, B.R., 2015, Gondolellid conodonts and depositional setting of the Phosphoria Formation. *Micropaleontology*, v. 61, pp. 335–368.
- Wardlaw, B.R., and Collinson, J.W., 1979, Biostratigraphic zonation of the Park City Group. In: Wardlaw, B.R. (Ed.), *Studies of the Permian Phosphoria Formation and related rocks, Great Basin-Rocky Mountain region*, Geological Survey Professional Paper, 1163D, pp. 17–21.
- Wardlaw, B.R., and Mei, S.L., 1999, Refined conodont biostratigraphy of the Permian and lowest Triassic of the Salt and Khizor Ranges, Pakistan. In: *Proceedings Proceedings of the International conference on Pangea and the Paleozoic-Mesozoic transition*, Wuhan, China University of Geosciences Press, pp. 154–156.
- Wardlaw, B.R., and Nestell, M.K., 2010, Latest Middle Permian conodonts from the Apache Mountains, West Texas. *Micropaleontology*, v. 56, n. 1–2, pp. 149–183.
- Wardlaw, B.R., and Nestell, M.K., 2015, Conodont faunas from a complete basinal succession of the upper part of the Wordian (Middle Permian, Guadalupian, West Texas). *Micropaleontology*, v. 61, pp. 257–292.
- Wignall, P.B., Sun, Y.D., Bond, D.P.G., Izon, G., Newton, R.J., Vedrine, S., Widdowson, M., Ali, J.R., Lai, X.L., Jiang, H.S., Cope, H., and Bottrell, S.H., 2009, Volcanism, mass extinction, and carbon isotope fluctuations in the Middle Permian of China. *Science*, v. 324, pp. 1179–1182.
- Wilde, G.L., 1975, Fusulinid-defined Permian stages. In: Cys, J.M., and Toomey, D.F. (Eds.), *Permian Exploration, Boundaries, and Stratigraphy*. Society of Economic Paleontologists and Mineralogists, West Texas Geological Society and Permian Basin Section, Publication, 75–65: Tulsa, Society of Economic Paleontologists and Mineralogists, pp. 67–83.
- Wilde, G.L., 1990, Practical fusulinid zonation: The species concept; with Permian Basin emphasis. *West Texas Geological Society Bulletin*, v. 29, pp. 5–34.
- Wilde, G.L., 2000, Formal Middle Permian (Guadalupian) series; a fusulinean perspective.. The Guadalupian symposium: Smithsonian Contributions to the Earth Sciences, v. 32, pp. 89–100.
- Wilde, G.L., Rudine, S.F., and Lambert, L.L., 1999, Formal designation: Reef Trail Member, Bell Canyon Formation, and its significance for recognition of the Guadalupian-Lopingian boundary. In: Saller, A.H., Harris, P.M., Kirkland, B.L., and Mazzullo, S.J. (Eds.), *Geologic framework of the Capitan Reef*. SEPM Special Publication, v. 65, pp. 63–84.
- Wu, Q., Ramezani, J., Zhang, H., Wang, T.T., Yuan, D.X., Mu, L., Zhang, Y.C., Li, X.H., and Shen, S.Z., 2017, Calibrating the Guadalupian Series (Middle Permian) of South China. *Palaeogeography, Palaeoclimatology, Palaeoecology*, v. 466, pp. 361–372.
- Wu, Q., Ramezani, J., Zhang, H., Yuan, D.X., Erwin, D.H., Henderson, C.M., Lambert, L.L., Zhang, Y.C., and Shen, S.Z., 2020, High-precision U-Pb zircon age constraints on the Guadalupian in West Texas, USA. *Palaeogeography, Palaeoclimatology, Palaeoecology*, v. 548, pp. 109668.
- Yang, J.H., Cawood, P.A., Du, Y.S., Condon, D.J., Yan, J.X., Liu, J.Z., Huang, Y., and Yuan, D.X., 2018, Early Wuchiapingian cooling linked to Emeishan basaltic weathering?. *Earth and Planetary Science Letters*, v. 492, pp. 102–111.
- Yuan, D.X., Shen, S.Z., Henderson, C.M., Lambert, L.L., Hearst, J.M., Zhang, Y.C., Chen, J., Qie, W.K., Zhang, H., Wang, X.D., Qi, Y.P., and Wu, Q., 2021, Reinvestigation of the Wordian-base GSSP section, West Texas, USA. *Newsletters on Stratigraphy*, v. 54, pp. 301–315.
- Zhang, B.L., Yao, S.P., Wignall, P.B., Hu, W.X., Liu, B., and Ren, Y.L., 2019, New timing and geochemical constraints on the Capitanian (Middle Permian) extinction and environmental changes in deep-water settings: evidence from the Lower Yangtze region of South China. *Journal of the Geological Society*, v. 176, pp. 588–608.
- Zhang, B.L., Yao, S.P., Mills, B.J.W., Wignall, P.B., Hu, W.X., Liu, B., Ren, Y.L., Li, L.L., and Shi, G., 2020, Middle Permian organic carbon isotope stratigraphy and the origin of the Kamura Event. *Gondwana Research*, v. 79, pp. 217–232.
- Zhang, G.J., Zhang, X.L., Li, D.D., Farquhar, J., Shen, S.Z., Chen, X.Y., and Shen, Y., 2015, Widespread shoaling of sulfidic waters linked to the end-Guadalupian (Permian) mass extinction. *Geology*, v. 43, pp. 1091–1094.
- Zhang, Y.C., and Wang, Y., 2018, Permian fusuline biostratigraphy. *Geological Society, London, Special Publications*, v. 450, pp. 253–288.
- Zhong, Y.T., He, B., and Xu, Y.G., 2013, Mineralogy and geochemistry of claystones from the Guadalupian-Lopingian boundary at Penglaitan, South China: Insights into the pre-Lopingian geological events. *Journal of Asian Earth Sciences*, v. 62, pp. 438–462.
- Zhou, M.F., Malpas, J., Song, X.Y., Robinson, P.T., Sun, M., Kennedy, A.K., Lesher, C.M., and Keays, R.R., 2002, A temporal link between the Emeishan large igneous province (SW China) and the end-Guadalupian mass extinction. *Earth and Planetary Science Letters*, v. 196, pp. 113–122.
- Zhou, Z.R., 2017, Permian basinal ammonoid sequence in Nanpanjiang area of South China-possible overlap between basinal Guadalupian and platform-based Lopingian. *Journal of Paleontology, Memoir* 91, S74, pp. 1–95.



**Shu-zhong Shen** is a Professor at the School of Earth Sciences and Engineering of Nanjing University and a Member of Chinese Academy of Sciences. He was the former Chair of the Subcommission on Permian Stratigraphy and the current Vice-Chair of the International Commission on Stratigraphy. His main research interests include Permian brachiopods, conodonts, biostratigraphy, diversity patterns, end-Permian mass extinction and environmental changes in deep time.



**Dong-xun Yuan** is an Associate Professor at the School of Resources and Geosciences, China University of Mining and Technology. He got his Ph.D. in geology of Nanjing University in 2015. His primary research focuses on the Permian conodonts, biostratigraphy, paleobiogeography and global correlation.



**Charles M. Henderson** is a Professor at the University of Calgary where he has taught stratigraphy and paleontology since 1989. His research focusses on global biostratigraphy of Permian and Early Triassic conodonts and completing the chronostratigraphic subdivisions of the Permian System. He is a Fellow of The Royal Canadian Geographical Society and the Geological Society of America and former Chairman of the Subcommission on Permian Stratigraphy, ICS.



**Xiang-dong Wang** is a Professor at the School of Earth Sciences and Engineering of Nanjing University. His research focuses on the Carboniferous and Permian stratigraphy, rugose corals, and Late Paleozoic Ice Age. He is the current Chairman of the Subcommission on Carboniferous Stratigraphy.



**Lance L. Lambert** is a Professor in the Department of Earth and Planetary Sciences, University of Texas at San Antonio. He has wide-ranging interests in paleoecology of the Late Paleozoic that include conodont and ammonoid biostratigraphy, as well as Carboniferous-Permian chronostratigraphy.



**Hua Zhang** is a Professor of the Nanjing Institute of Geology and Palaeontology, Chinese Academy of Sciences. His main research interests include the deep-time biogeochemistry and palaeoenvironmental changes and end-Permian mass extinction.



**Yi-chun Zhang** is a Professor at the Nanjing Institute of Geology and Palaeontology, Chinese Academy of Sciences. His research focuses on taxonomy, biostratigraphy and paleobiogeography of Permian foraminifers.



**Qiong Wu** is a postdoctoral at the School of Earth Sciences and Engineering of Nanjing University. Her research interest includes the application of high-precision U-Pb geochronology by LA-ICPMS, SIMS and CA-ID-TIMS techniques to chronostratigraphy of marine and terrestrial sediments and calibration of various geological and biological events.



**Douglas H. Erwin** is a Senior Scientist at the National Museum of Natural History (Smithsonian) in Washington DC, and a research professor at the Santa Fe Institute in Santa Fe, New Mexico. In addition to the Permo-Triassic, his other research interests include macroevolutionary dynamics and the radiation of animals during the Ediacaran-Cambrian.



**Wen-qian Wang** is a postdoctoral at the School of Earth Sciences and Engineering of Nanjing University. Her current research interest is mainly on isotopic geochemistry, palaeoenvironment and palaeoclimate using brachiopod shells and conodonts.



**Jahan Ramezani** is a Research Scientist at the Massachusetts Institute of Technology. He is interested in high-precision U-Pb geochronology applied to the stratigraphic record and geologic history. His research focuses on calibration of the geologic time scale and co-evolution of Earth and life in deep time.



**Jonena M. Hearst** is a Geologist at the National Park Service of the Guadalupe Mountains National Park in Texas. She is pointing the GSSP marker of the base of the Capitanian Stage at Nipple Hill.



**Jun Chen** is an Assistant Professor at the Guangzhou Institute of Geochemistry, Chinese Academy of Sciences (GIGCAS). His current research includes conodont biostratigraphy, palaeotemperature reconstruction using conodont apatite, and environmental and biological impact of large igneous provinces.



**Yuping Qi** is a Research Professor at the Nanjing Institute of Geology and Palaeontology, Chinese Academy of Sciences. His research interests include the Carboniferous and Cambrian biostratigraphy and systematics of conodonts. He mainly focuses on the Carboniferous GSSPs in South China during the recent five years.



**Yue Wang** is a Professor at the Nanjing Institute of Geology and Palaeontology, Chinese Academy of Sciences. Her research interests include Permian stratigraphy, systematics and evolution of fusulines, and biological events in response to the climatic transition from icehouse to greenhouse during the Permian.



**Bruce R. Wardlaw** was the former Chief Paleontologist of the US Geological Survey. He was an internationally well-known expert in Paleozoic fossils and stratigraphy, especially in Permian conodonts. He served as the Chair of the Subcommission on Permian Stratigraphy between 1996-2004. He passed away on March 23, 2016.



**Wen-kun Qie** is a Professor at the Nanjing Institute of Geology and Palaeontology, Chinese Academy of Sciences. His current research interests include carbonate sedimentology, stable isotope geochemistry and integrative stratigraphy of Devonian and Carboniferous in China.